Austrian Journal of Technical and Natural Sciences

№ 7–8 2022
July – August

PREMIER
Publishing

Vienna
2022

Austrian Journal of Technical and Natural Sciences

Scientific journal

№ 7 – 8 2022 (July – August)

ISSN 2310-5607

Editor-in-chief Hong Han, China, Doctor of Engineering Sciences

International editorial board

Andronov Vladimir Anatolyevitch, Ukraine, Doctor of Engineering Sciences
Bestugin Alexander Roaldovich, Russia, Doctor of Engineering Sciences
S.R.Boselin Prabhu, India, Doctor of Engineering Sciences
Frolova Tatiana Vladimirovna, Ukraine, Doctor of Medicine
Inoyatova Flora Ilyasovna, Uzbekistan, Doctor of Medicine
Kambur Maria Dmitrievna, Ukraine, Doctor of Veterinary Medicine
Kurdzeka Aliaksandr, Russia, Doctor of Veterinary Medicine
Khentov Viktor Yakovlevich, Russia, Doctor of Chemistry
Kushaliyev Kaisar Zhalitovich, Kazakhstan, Doctor of Veterinary Medicine
Mambetullaeva Svetlana Mirzamuratovna, Uzbekistan, Doctor of Biological Sciences
Manasaryan Grigoriy Genrihovich, Armenia, Doctor of Engineering Sciences
Martirosyan Vilena Akopovna, Armenia, Doctor of Engineering Sciences
Miryuk Olga Alexandrovna, Kazakhstan, Doctor of Engineering Sciences
Nagiyev Polad Yusif, Azerbaijan, Ph.D. of Agricultural Sciences
Nemikin Alexey Andreevich, Russia, Ph.D. of Agricultural Sciences
Nenko Nataliya Ivanovna, Russia, Doctor of Agricultural Sciences
Ogirko Igor Vasilievich, Ukraine, Doctor of Engineering Sciences
Platov Sergey Iosifovich, Russia, Doctor of Engineering Sciences
Rayiha Amenzade, Azerbaijan, Doctor of architecture
Shakhova Irina Aleksandrovna, Uzbekistan, Doctor of Medicine
Skopin Pavel Igorevich, Russia, Doctor of Medicine
Suleymanov Suleyman Fayzullaevich, Uzbekistan, Ph.D. of Medicine
Tegza Alexandra Alexeevna, Kazakhstan, Doctor of Veterinary Medicine
Zamazy Andrey Anatolievich, Ukraine, Doctor of Veterinary Medicine
Zhanadilov Shaizinda, Uzbekistan, Doctor of Medicine

Proofreading Kristin Theissen

Cover design Andreas Vogel

Additional design Stephan Friedman

Editorial office Premier Publishing s.r.o.
Praha 8 – Karlín, Lyčkovo nám. 508/7, PSČ 18600

E-mail: pub@ppublishing.org

Homepage: ppublishing.org

Austrian Journal of Technical and Natural Sciences is an international, German/English/Russian language, peer-reviewed journal. It is published bi-monthly with circulation of 1000 copies.

The decisive criterion for accepting a manuscript for publication is scientific quality. All research articles published in this journal have undergone a rigorous peer review. Based on initial screening by the editors, each paper is anonymized and reviewed by at least two anonymous referees. Recommending the articles for publishing, the reviewers confirm that in their opinion the submitted article contains important or new scientific results.

Premier Publishing s.r.o. is not responsible for the stylistic content of the article. The responsibility for the stylistic content lies on an author of an article.

Instructions for authors

Full instructions for manuscript preparation and submission can be found through the Premier Publishing s.r.o. home page at:
http://ppublishing.org.

Material disclaimer

The opinions expressed in the conference proceedings do not necessarily reflect those of the Premier Publishing s.r.o., the editor, the editorial board, or the organization to which the authors are affiliated.

Premier Publishing s.r.o. is not responsible for the stylistic content of the article. The responsibility for the stylistic content lies on an author of an article.

Included to the open access repositories:

© Premier Publishing s.r.o.

All rights reserved; no part of this publication may be reproduced, stored in a retrieval system, or transmitted in any form or by any means, electronic, mechanical, photocopying, recording, or otherwise, without prior written permission of the Publisher.

Typeset in Berling by Ziegler Buchdruckerei, Linz, Austria.
Printed by Premier Publishing s.r.o., Vienna, Austria on acid-free paper.

Section 1. Technical sciences

Ahttps://doi.org/10.29013/AJT-22-7.8-3-7

Turmanova Oralkhan Kalbaevna,
Associate Researcher, Karakalpak Research Institute of Natural Sciences, Karakalpak Branch of the Academy of Sciences RUz, Nukus
Allaniyazov Davran Orazymbetovich,
Doctor of Technical Sciences, (PhD) Karakalpak Research Institute of Natural Sciences of the Karakalpak Branch of the Academy of Sciences RUz, Nukus
Bauatdinov Tashkentbay Salievich,
Doctor of Technical Sciences, (PhD) Karakalpak Institute of Agriculture and Agrotechnology, Nukus;
Dilmanova Nargiza Abdirazakovna,
Associate Researcher, Karakalpak Research Institute of Natural Sciences, Karakalpak Branch of the Academy of Sciences RUz, Nukus
Saparniyazov Berdak Abdirazakovich,
master's student of the Nukus branch of the Tashkent University of Information Technologies named after Muhammad Al-Khorazmiy

STUDY OF SALINITY OF SOILS IN SOME AREAS OF KARAKALPAKSTAN

Abstract. Studies were carried out to assess the state of soils in the Muinak, Chimbay and Amu Darya districts for salinization and content of water-soluble salts in the Muinak, Chimbay and Amu Darya districts. All soil samples taken are saline, saline-sulfate-chloride, chloride-sulfate, sulfate. The degree of salinity varies from medium to very strong in all soil profiles. Summary data on the studied components, the most characteristic soil conditions of the surveyed areas are also provided.

Keywords: Salination of soils, soils, salinity, emptying, salts, agriculture, water-soluble salts, loam.

Introduction. The anthropogenic factor led to a violation and change in the natural conditions of the Southern Aral Sea. The changes affected all components of the natural environment, primarily surface and groundwater. Then the restructuring of the natural environment affected the soils, causing the process of their salinization and desertification. Changing the environmental situation causes damage, manifested in the reduction of soils suitable for agriculture, and a decrease in land productivity. The process of draining and drying the bottom of the Aral Sea led to pollution, the environment, salinity of soils, salinity, which depends on the areas of phased salt formations [1].

The adaptability of plants to salts arose in the process of evolution during the development of saline habitats by plants. It has also been found that long-term cultivation of plants on saline soil in combination with selection leads to a significant increase in salt resistance.

Under the salt resistance of crops, those limit values of salt content are taken, at which normal growth, development and ability to yield crops are possible. Plants adapted to soil settlement are distinguished not only by high salt resistance, but also by an increase in productivity.

Research objects and methods. The object of the study in this work is the soils of the Muynak district: the Ali aul site located 80 km from the center of Muynak, the Dustlik site 70 km from the center of Muynak. The soils of the Chimbay and Amu Darya districts were also studied.

Research material and methodology. Water extract of soils was prepared according to the generally accepted method-soil: water in ratio 1:5 [2]. The content of chlorine ions was determined by argentometric methods by sea; calcium and magnesium trilonometric; sulfate by titration; aqueous drawing with a sulfuric acid solution in the presence of a methyl orange indicator; sodium and potassium ions by the difference in the sum of anions and cations. The results of the analysis of aqueous extracts were expressed in milligram equivalents per 100 g of dry air soil, the sum of water-soluble salts in percent.

The results of the aqueous extract analysis were monitored for a dense (dry) residue.

The degree of soil salinization was assessed on a scale of [2–4].

Table 1. – Content of water-soluble salts of the Ali aul site in the Muynak region

	section No.	depth. cm	dry residue.%	CO_3 in%	the general HCO_3 in%	Ce^-%	SO_4^-%	Ca%	Mg%	Na+K by difference		Sum of components. in%
										mg/eq	in%	
-S- strongly	Light loam	0–10	2.231	–	0.049	0.142	1.248	0.170	0.024	20.3	0.467	2.100
-S-strongly	loam	10–20	2.217	–	0.061	0.142	1.224	0.180	0.018	20.0	0.460	2.085
-S-so-so	sandy loam	20–40	1.676	–	0.049	0.053	0.996	0.020	0.055	17.55	0.404	1.577
-Ch-S-so-so	sandy loam	40–60	0.560	0.001	0.029	0.071	0.269	0.106	0.016	1.52	0.035	0.527
-Ch-S-so-so	sandy loam	60–80	0.396	–	0.024	0.057	0.187	0.028	0.029	2.1	0.048	0.373

Table 2. – Content of water-soluble salts of the Dustlik section of the Muynak region

	section No.	depth, cm	dry residue,%	CO_3 in%	the general HCO_3 in%	Ce^-%	SO_4^-%	Ca%	Mg%	Na+K by difference		Sum of components, in%
										mg/eq	in%	
-S-so-so	loam	0–10	1.632	–	0.073	0.071	0.912	0.140	0.012	14.2	0.327	1.535
-S-so-so	loam	10–20	2.063	–	0.110	0.106	1.104	0.180	0.024	16.8	0.420	1.944
-S-so-so	loam	20–40	1.614	–	0.073	0.071	0.900	0.135	0.012	14.2	0.327	1.614
-S-so-so	Clay	40–60	1.602	–	0.079	0.071	0.888	0.140	0.012	13.8	0.317	1.507
-S-so-so	Clay	60–80	1.596	–	0.085	0.071	0.876	0.145	0.006	13.9	0.320	1.503

Table 3. – Content of water-soluble salts of the Kenes section of the Chimbay region

	section No.	depth, cm	dry residue,%	CO_3 in%	the general HCO_3 in%	Ce^-%	SO_4^-%	Ca%	Mg%	Na+K by difference		Sum of components, in%
										mg/eq	in%	
-S-poorly	loam	0–10	1.247	–	0.031	0.089	0.708	0.060	0.061	9.75	0.224	1.173
-S-poorly	loam	10–20	1.240	–	0.037	0.089	0.696	0.065	0.058	9.6	0.221	1.166
-S-poorly	loam	20–40	1.229	–	0.043	0.089	0.684	0.070	0.058	9.2	0.212	1.156
-S-poorly	Light loam	40–60	1.403	0.002	0.029	0.021	0.207	0.032	0.001	3.76	0.087	0.379
-S-so-so	Light loam	60–80	1.958	–	0.055	0.071	0.516		0.049	5.65	0.130	0.958

Table 4. – Content of water-soluble salts of the Aiteke site in the Chimbay region

	section No.	depth, cm	dry residue,%	CO_3 in%	the general HCO_3 in%	Ce^-%	SO_4^-%	Ca%	Mg%	Na+K by difference		Sum of components, in%
										mg/eq	in%	
-Ch-S-so-so	Light loam	0–10	0.552	–	0.022	0.064	0.288	0.088	0.033	1.06	0.224	0.519
-Ch-S-so-so	Light loam	10–20	0.548	–	0.024	0.064	0.283	0.090	0.030	1.1	0.225	0.516
-S- poorly	loam	20–40	0.714	–	0.029	0.028	0.413	0.020	0.026	6.78	0.156	0.672
-S-poorly	loam	40–60	0.711	–	0.032	0.028	0.408	0.022	0.024	6.72	0.155	0.669
-S-poorly	loam	60–80	0.707	–	0.034	0.028	0.403	0.024	0.023	6.66	0.153	0.665

Table 5. – Content of water-soluble salts of the Kilichboy site in the Amu Darya region

	section No.	depth, cm	dry residue,%	CO_3 in%	the general HCO_3 in%	Ce^-%	SO_4^-%	Ca%	Mg%	Na+K by difference		Sum of components, in%
										mg/eq	in%	
-S- ery much	loam	0–10	3.075	–	0.061	0.213	1.848	0.411	0.243	5.0	0.115	2.891
-S-strongly	loam	10–20	3.039	–	0.073	0.213	1.680	0.301	0.085	20.2	0.505	2.857
-S-strongly	loam	20–40	2.217	–	0.061	0.142	1.224	0.180	0.018	20.0	0.460	2.085
-S-poorly	Clay	40–60	0.714	–	0.027	0.028	0.446	0.014	0.078	3.44	0.079	0.672
-S-poorly	Clay	60–80	0.712	–	0.029	0.028	0.442	0.018	0.075	3.38	0.078	0.670

Research results: Soil salinization occurring in arid regions is associated with the predominance of water evaporation over soil washing processes. Water found in the lower horizons ascends the soil

capillaries to the surface, water evaporates, and salts remain in the upper soil layers.

During winter, the salts are backwashed deep into the soil. In addition to this factor, arid salinity occurring in the zone of the Southern Aral Sea also imposes an imprint on the state of soils.

The amount of soils salted to varying degrees in the Southern Aral region is almost 95%, and in the Muinak territory, the most close to the Aral ecological crisis zone is 99% [5]. Therefore, crop production under harsh conditions in the Southern Aral Region (saline soils, a sharply continental climate with sharp temperature fluctuations, water scarcity) determines the choice of a scientific approach to assessing the types and salinity of soils, their reclamation state, the development of methods for their processing, the selection of the most salt-resistant and drought-resistant crops, methods for increasing their salt resistance for successful harvest.

Among the cultivated plants there are some plants that are relatively well tolerant of the high salt content in the soil. These are sugar beets and cotton [3].

Scientists of the Karakalpak Research Institute of Natural Sciences KKOANRUz conducted research in the Muinak, Chimbai and Amu Darya districts to assess the state of soils.

40 soil samples were analyzed. According to the results of the studies, it was established that the soils differentiate in terms of grain size distribution. The horizons are composed of both sands and fine soil-clay fractions, loams. Throughout the soil, there are salts that allow only the most salt-tolerant crops to grow.

The table summarizes the studied components, the most characteristic soil conditions of the surveyed areas.

The site is classified as highly saline and mechanically classified as loam.

The upper horizons are characterized by a sulfate type of salinization, and the lower chloride-sulfate type of salinization and the mechanical composition belong to sandy loams. Sunflower, sugar beets, feed beets, technical sorghum, ordinary sorghum can grow in such areas as having the highest degree of salt resistance.

The site belongs to the category of very highly saline, mechanically to loams and clays. Therefore, it is necessary to carry out reclamation and agrotechnical measures.

The upper horizons are characterized by the chloride-sulfate type of salinization, and the lower – sulfate type of salinization. Sunflower with the highest degree of salt resistance can grow in such areas.

The site belongs to the category of strongly and very strongly salted, and mechanically to loams.

On the first table: upper horizons (0–10 cm), (10–20 cm), medium horizons (20–40 cm) are characterized by sulfate type of salinization, horizon 40–60 cm, 60–80 cm are characterized by chloride-sulfate type of salinization.

On the second, third and fifth table: all horizons are of sulfate type of salinization, and on the fourth table: the upper (0–10 cm, 10–20 cm) are characterized by chloride-sulfate type of salinization, the horizon is 20–40 cm, 40–60 cm, 60–80 cm are characterized by sulfate type of salinization.

With regard to sandy soils, maximum precautions must be taken. The slightest mechanical effect on the soil can cause negative phenomena: intense deflation, aeolian removal of salts.

Conclusions: Thus, studies have shown that all soil samples are saline, characterized by mixed salinization-chloride-sulfate, the sulfate degree of salinization varies from medium to very strong in all soil profiles.

It was revealed that the soils differ in their mechanical composition and degree of salinity, which indicates the need to develop special rules for the selection and preparation of planting zones and crops to increase their engraftment. Various agrotechnical activities significantly wander on the growth and development of agricultural plants.

In addition to combating soil salinization by selecting crops and creating salt-resistant varieties, it is necessary to apply techniques to certain types of soil salinization that ensure increased salt resistance and yield of cultivated plants on salinized soils.

References:

1. Turemuratova A. S., Reimov K. D., Allaniyazov D. O. Distribution of salts in groundwater and the drained surface of the Aral Sea. Universum: Chemistry and Biology,– No. 6–1 (96). 2022.– P. 31–36.
2. Arinushkina E. V. Manual on chemical analysis of soils.– M.: Moscow State University Publishing House, 1970.– 257 p.
3. Henkel P. A. Plant physiology.– M.: Enlightenment, 1975.– P. 140–208.
4. Kovda V. A. Problems of combating desertification and salinization of irrigated soils.– M.: Kolos, 1984.– 304 p.
5. Khufler F., Massino I. V., Mambetnazarov B., Edenbaev D. Our work in agricultural areas of the Southern Aral Sea.– Tashkent, 2002.– P. 12–13.

https://doi.org/10.29013/AJT-22-7.8-8-11

Deryaev Annaguly Rejepovich,
Candidate of Technical Sciences, Senior Researcher,
Scientific Research Institute of Natural Gas
of the State Concern „Turkmengas", Ashgabat, Turkmenistan

PROTECTION OF THE SUBSOIL AND THE ENVIRONMENT DURING THE DEVELOPMENT OF GAZ FIELDS BY DUAL COMPLETION

Abstract. The development of an oil field as a whole and each of its individual objects should be carried out in accordance with approved project documents. Proposals made during the operation of a field (deposits) that are not foreseen by the project (technological scheme) to improve the development system, leading to changes in the accepted design provisions on the number of producing and injection wells, oil production levels and water injection, can be initiated by implementation only after the project document is re-approved.

Industrial development of oil and oil and gas fields is allowed only if the gas extracted together with oil is used in the national economy or, for temporary storage purposes, is pumped into special underground storage facilities, into oil reservoirs being developed or to be developed.

In the process of industrial development of oil fields, the collection and use of gas, condensate and related valuable components and water extracted together with oil must be ensured in the volumes provided for in the approved technological project document. A project for the development of an oil field for industrial development can be accepted for approval only if it solves the issues of collecting and rational use of petroleum gas.

Keywords: exploration, development, oil production, pollution, catastrophe, flora, fauna, soil erosion.

The issues of ecology and nature protection include restrictions on the external impact on the environment, preventing the loss of hydrocarbon resources during the extraction, carrying out technical and control measures.

Oil and gas enterprises occupy one of the first places among other sectors of the national economy in terms of the degree of environmental impact. Exploration and development of oil fields includes such technologies as exploration drilling, oil production, collection and preparation of hydrocarbons, transportation and processing.

The enterprises of the oil and gas industry have a harmful effect on all objects of nature, the atmosphere, the hydrosphere and underground and surface waters, the geological environment, drilled wells at all depths, on the land where they are located.

The cycle of oil and gas works consists of two main groups:

1. New construction sites (search and exploration, drilling, installation of equipment).

2. Working processes of the enterprise (collection, processing, shipment and processing of oil and gas).

When carrying out construction work, a report is made on technogenic pollution of the earth and the environment for technical reasons.

A report on the measures taken to protect the environment should be prepared by oil and gas producing organizations [1].

It should be noted that the time spent on exploration, drilling and preparation of oil and gas fields, the production time of the enterprise, pollution is caused for technical reasons.

The performance of these works causes high harm to the environment. Ecological catastrophes that occur are physical and mechanical impacts on soil, land, flora, fauna, soil, lowering of hydrogeological conditions, strengthening of soil erosion conditions, deterioration of living conditions of fauna and flora and local residents, and others.

Currently, geological studies have been completed at the Altyguyi gas condensate field and a field test plan has been prepared based on the data obtained.

When drilling wells in the fields, the environment is polluted mainly by some chemical elements used in the preparation of drilling fluids.

Currently, normal limit values, chemical elements indicating aggressiveness used in the preparation of drilling fluids have not been established.

During drilling operations, the source of atmospheric air pollution is diesel-fueled equipment that emits 2 tons of hydrocarbons and soot, 30 tons of nitrogen oxides, 8 tons of carbon monoxide and 5 tons of sulfur anhydrite into the atmosphere during the year. When drilling wells, drilling mud is mixed with soil layers, surface and groundwater, forming 30 m^3/day of water used [2].

During the development of wells, hydrocarbon mainly causes pollution. In most cases, oil-based circulating solutions with serious environmental consequences produce used wastewater, suspension and colloidal solution.

When preparing environmental protection measures during installation work in wells, it is necessary to avoid work that negatively affects natural objects. Since the sources of pollution are closely related to the technology used by the enterprise, it is necessary to establish the technology that has the least impact on the environment. When geochemical breakdown of the soil, it is necessary to perform the following:

– When preparing plots, it is necessary to prevent contamination of the topsoil from the products obtained;

– To collect sedimentary rocks of drilled rocks on slurry barns;

– It is necessary to cover the slurry barn;

– Restore the soil area of the extracted products;

– Road construction.

As a result of drilling operations, there is a negative impact on the hydrogeological change in the soils of the earth, and as a result, drilling fluids penetrate into aquifers, which lead to the formation of a complex of waters.

The waters used in drilling fluids are divided into three groups:

1. Water formed during the production of works;

2. Water for household work;

3. Atmospheric, rainwater.

Circulating waters are used to carry drilled rocks to the surface. In world practice, 95% of clay elements are mixed into the composition of circulating waters for the preparation of drilling fluids.

The quality of the flushing solutions used helps the speed of drilling operations, the prevention of complications with colmatation and water occurrence [3].

During the operation of producing wells and oil and gas collection facilities, the integrated safety and environmental protection system includes:

– monitoring of the condition of borehole fittings;

– selection of equipment and pipelines that meet the specified operating conditions, taking into account current regulations;

– periodic testing of equipment for strength (crimping);

– corrosion protection;

– prevention of technological complications that create emergency situations (gas communications flooding, deposition of paraffin and salts in wells and collection systems), with the use of special inhibitor substances.

When collecting and storing oil, the requirement of safety and reduction of hydrocarbon emissions into the environment are ensured at the stage of arming assembly points in compliance with building codes and regulations, with the necessary equipment of tanks with floating roofs or breathing valves, with mandatory collapse of tank farms to localize emergency oil spills [4].

When implementing the gas lift method of oil production, with a high manifestation of gas injected into the well to ensure safety and environmental protection, it is envisaged (in addition to the design and construction of the main facilities in full compliance with the required technological parameters of operation according to the current building codes and regulations) the construction and proper operation of additional technological equipment that provides a hydrate-free operation of gas distribution systems (furnaces for heating gas and inhibition unit). In the case of the construction of furnaces for heating hydrocarbons, make a preliminary calculation of atmospheric pollution by combustion products and assess the need to determine the MPC.

Storage and use of chemicals is planned to be carried out in accordance with their individual characteristics and in accordance with Safety Regulations (SR) in the oil industry, including providing employees with personal protective equipment (PPE), carrying out instructions and monitoring the condition of equipment used for the use of chemicals (surfactants, methanol, etc.).

The operation of electrical installations and heating equipment is provided in accordance with the current rules of SR and fire safety rules.

According to estimates, in oil fields with a similar technology of oil extraction and collection, the maximum concentrations of the above harmful substances at the border of the sanitary zone (within a radius of 1000 m from the source of emission) do not exceed the maximum permissible (MPC), which are set for each harmful substance individually according to the methodology of the State Committee for Hydrometeorology (OND-86).

In this regard, emissions of harmful substances into the atmosphere, subject to regular (accident-free) technological modes of operation of oil and gas field equipment, can be considered approximately corresponding to the maximum permissible emissions (MPI) [5].

A detailed assessment of emissions for all fishing facilities is taken into account when compiling an environmental passport.

The environmental passport is being developed in accordance with GOST 17.0.0.04–90 "System of standards in the field of nature protection and improvement of the use of natural resources", which already gives the full technological cycle of this production from the supply of raw products to the finished product. At the same time, the presence of emissions, discharges and solid waste is carefully checked and calculated at each production facility and their impact on the environment is analyzed. All this material is described and calculated in the relevant chapters of the environmental passport. It also concludes that it is necessary to calculate the norms of MPD, the results of which are issued in the form of a second volume, but in the future, in the event of an increase in oil production due to Miocene-Paleogene and Mesozoic underlying red-colored sediments, it will be necessary to adjust all calculations on emissions.

References:

1. Деряев А. Р. Рекомендации по буровому раствору для бурения секции 215,9 мм открытого ствола наклонно-направленной скважины. // Сборник статей II Международной научно-практической конференции "Наука, общество, технологии: проблемы и перспективы взаимодействия в современном мире".– Петрозаводск: Научное издание: МЦНП "Новая наука". 2022.– С. 17–22.

2. Деряев А. Р. Рекомендации по борьбе с поглощением при бурении наклонно-направленных скважин. // Сборник статей Международной научно-практической конференции “Инструменты и механизмы современного инновационного развития” – Уфа: Издательство ООО “Омега скайнс”. 2022.– С. 62–65.
3. Деряев А. Р. Обоснование принятой методики прогноза технологических показателей разработки нефтяных и нефтегазовых залежей // Научный журнал “IN SITU” № 5/2022 – М: Академическое издательство: “Научная артель”. 2022.– С. 24–26.
4. Деряев А. Р. Охрана недр и окружающей среды при разработке газовых месторождений методом одновременной раздельной эксплуатации // Научный журнал Метод Z № 2(4) – Санкт-Петербург: Издательство: ГНИИ «Нацразвитие». 2022.– С. 12–14.
5. Deryýaýew A. R., Jamiýew M. Ý., Gulatarow H., Mantrowa S. W. Çäklendirilen patent: „Toýunly ergini ingibirlenen termostabilleşdirilen goşundy KAIR-T bilen işläp bejermegiň usuly“. 06.06.2014 ý. senede döwlet tarapyndan reýestre bellige alnan № 604 belgili patent.

https://doi.org/10.29013/AJT-22-7.8-12-15

Murtazaev A. M.,
Candidate of technical sciences, Professor,
Tashkent State Technical University
Raupov A. A.,
PhD, Associate Professor,
Tashkent State Technical University
Sokhibov D. Z.,
Basic doctoral student,
Tashkent State Technical University

STUDY OF THE PROPERTIES OF MODIFIED DEXTRIN MIXTURES FOR DRILLING

Abstract. In the article, the structure of modified dextrin obtained in different proportions was studied by means of IR-spectroscopy, SEM analysis, and its physical and chemical properties were analyzed. Modified dextrin, which forms the basis of the new composition of the obtained drilling mixtures, allows to use them in oil and gas wells at different pressures and temperatures.

Keywords: mineral powder (calcium carbonate), modified dextrin, IR-spectroscopy, electron microscope analysis, drilling mixtures.

Introduction. The production of modified dextrin in the world and its use in food, pharmaceuticals, and industry increased to 2,785 million US dollars in 2020, and according to experts, it is predicted to grow to 4,032 million US dollars by 2030 [1].

When ordinary starch containing 10–20% water is exposed to different temperatures, with the help of special catalysts, starch molecules consisting of high-molecular natural polymers are broken down into low-molecular polymers, resulting in dextrin, which is more than 95% soluble in water at 20 °C [2; 3; 4; 5].

Chemical reagents containing modified starch, KMK and dextrin are widely used for drilling mixtures in the oil and gas industry to reduce water loss during drilling. The use of these drilling compounds strengthens the walls of the wells and serves to suppress the solid phase in the solution. This organic product is sensitive to the action of microorganisms, so it requires the addition of bactericidal additives [6; 7].

Discussion of the results. Exploration of hydrocarbon products and drilling in high temperature and pressure conditions are becoming more difficult. This situation was caused by the deterioration of the underground layer due to the inefficiency of the rheological properties of the fluids of the drilling mixtures due to the change in the pressure and temperature during the drilling process due to the decrease in the reserves of oil and gas products, the failure of the pipelines, the change of the shale layers, and the complication of the technological processes due to the high pressure. In order to overcome these problems, today, as a result of the use of modified starch-based drilling fluids, the fact that they have properties such as pressure, normalization of aquifers, and control of the density of the mixture creates an opportunity for scientific research and the development of effective technologies in this field [8; 9; 10].

In order to obtain and widely use the modified dextrin offered by us in drilling, the production enterprises of «Uzkimyosanoat» JSC focus on the

preparation of mixtures consisting of compounds containing metal, phosphorus, and nitrogen, which are necessary for the production of local raw materials – starch contained in rice husks.

Dextrin is mainly mixed with starch treated with hydrochloric acid. Then it is stored for 5–6 hours and modified for 2.5–5 hours in an oven or using an extruder at a temperature of 100–180 °C. The degree of dextrinization is determined by the color of the product: light yellow dextrin is 82–85% soluble in water, and orange color is a completely water-soluble product.

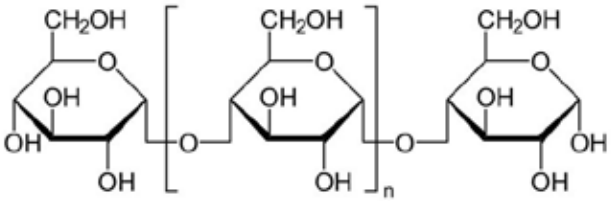

Figure 1. General structural formula of dextrin

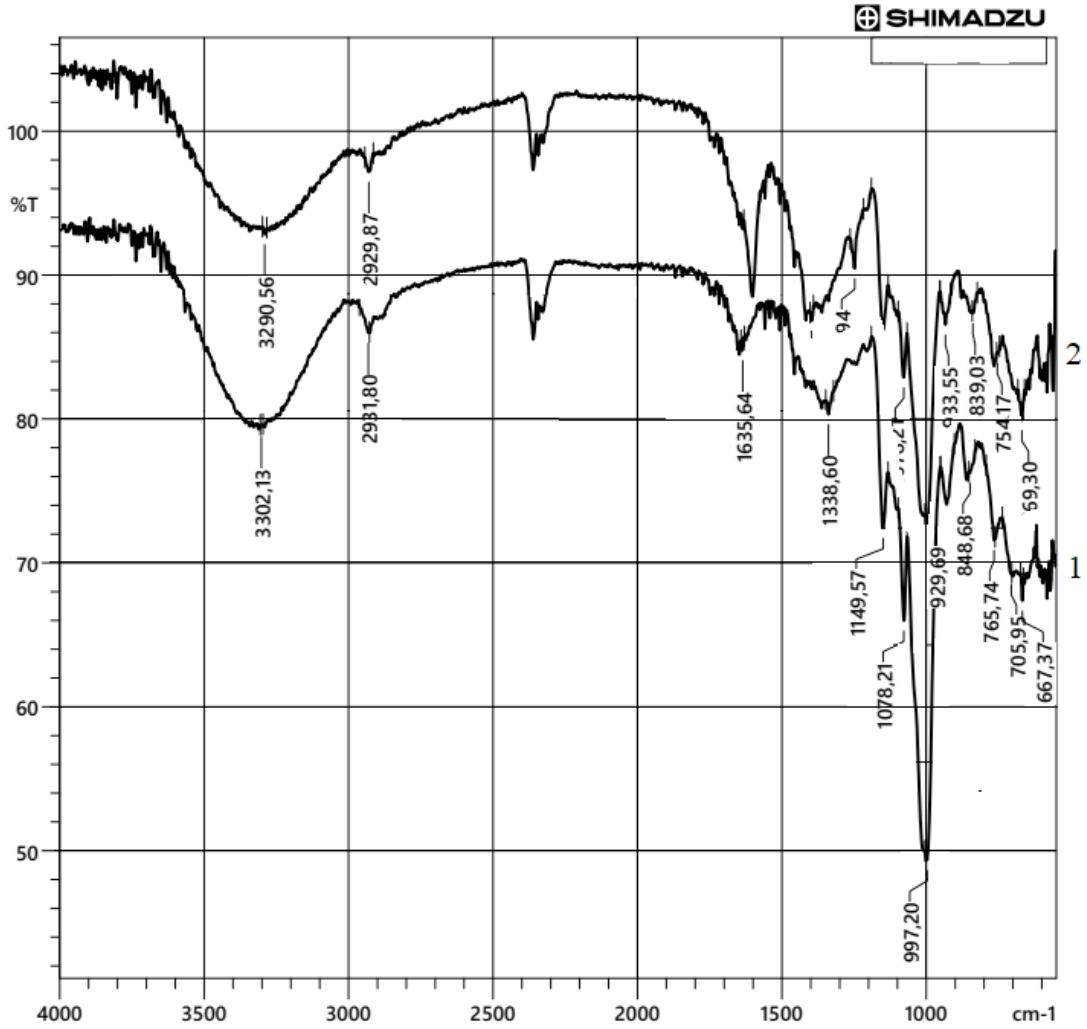

Figure 6. IR spectroscopy: (1) starch, (2) from the right

Figure 1 shows the IR spectroscopy of the obtained dextrin, mainly starch and hydroxyl groups in dextrin showed peaks in the range of 3310–3290 cm $^{-1}$. In addition, frequencies related to the S-N group were observed in the range of 2935–2920 cm^{-1}. It can be seen that the frequency in the region of 1100–1000 cm^{-1} is characteristic of the SN2-O-SN2 group in starch and dextrin, showing valence and valence bands. In IR-spectroscopy of dextrin and starch, frequencies were determined in several different regions. According to it, two new peaks at 1600–1150 cm^{-1} in dextrin were found to belong to the SOO-group.

Table 1. – Properties of the resulting dextrin

Characteristics of Namkna	Properties of dextrin obtained under the influence of temperature up to 100–180 °C		
	1	2	3
Processing temperature, °C	110	150	175
Solubility in water,%	73	76	85
Colour	Pale yellow	Orange	Dark orange
Density, г/см^3	1.03	1.03	1.02

Some physicochemical properties of dextrin obtained by processing starch at different temperatures are presented in (Table 1) below.

On the basis of the dextrin obtained in this way, the following composition was selected for the preparation of a mixture widely used in drilling oil and gas wells: mass%.

Dextrin	2–3
Oxidized starch	2–5
mineral powder (calcium carbonate)	25–30
clay mixture	10–15
sodium chloride	30–40
water	30–50

Conclusions. In the preparation of this composition, water is added until the mixture is formed, and mineral powder (calcium carbonate) and clay mixture are mixed. The mixing process was mixed at 3000 min/speed for 20–30 min. The finished oil and gas well drilling mixture is then allowed to stand for 24 hours and then mixed. To control the fluid viscosity of the resulting mixtures, a saturated solution of sodium chloride salt was added and stirred for 40 minutes, and if the viscosity increased, it was diluted by adding water.

Thus, dextrin, mineral powder (calcium carbonate) and clay mixture were added and mixed, and mineralization of drilling mixtures using mineral powder (calcium carbonate) and clay mixture allows to create new compositions of temperature stable drilling mixtures.

References:

1. Dextrin Market by Type and Application: Global Opportunity Analysis and industry Forecast, 2021–2030. URL: https://www.alliedmarketresearch.com/dextrin-market-A13097
2. Wever D., Picchioni F., Broekhuis A. Polymers for enhanced oil recovery: a paradigm for structure–property relationship in aqueous solution. Prog Polym Sci – 36: 2011.– P. 1558–16282.
3. Al-Muntasheri G., Nasr-El-Din H., Hussein I. A rheological investigation of a high temperature organic gel used for water shut-off treatments. J Pet Sci Eng – 59(1–2): 2007.– P. 73–83.
4. Olivia V. López, Luciana A. Castillo Mario D. Ninago, Andrés E. Ciolino, and Marcelo A. Villar. Modified Starches Used as Additives in Enhanced Oil Recovery (EOR) // See discussions, stats, and author profiles for this publication at: URL: https://www.researchgate.net/publication/319083538/ Chapter August, 2017. – P. 227–233. DOI: 10.1007/978–3–319–61288–1_9.
5. Aboulrous A. A., Mahmoud T., Alsabagh A. M., Abdou M. I. Application of natural polymers in engineering. In: Olatunji O (ed) Natural polymers: industry techniques and applications. Springer International Publishing, Cham. 2016.– P. 185–218.
6. Adewole J. K., Sultan A. S. A study on processing and chemical composition of date pit powder for application in enhanced oil recovery. Defect Diffusion Forum – 353: 2014.– P. 79–83.

7. Aliyu Adebayo Sulaimon. Evaluation of drilling muds enhanced with modified starch for HPHT well applications // Received: 23 July 2019 / Accepted: 17 October 2020. Journal of Petroleum Exploration and Production Technology. URL: https://doi.org/10.1007/s13202–020–01026–9.
8. Ghazali N. A., Alias N. H., Mohd T. A.T., Adeib S. I., Noorsuhana M. Y. Potential of corn starch as fluid loss control agent in drilling mud. Appl. Mech. Mater.– 754–755. 2015.– P. 682–687.
9. Soto D., Urdaneta J., Pernía K., León O., Muñoz-Bonilla A., Fernandez-García M. Removal of heavy metal ions in water by starch esters.– Starch-Starke.– 68. 2016.– P. 37–46.
10. Agbasimalo N., Radonjic M. Experimental study of the impact of drilling fluid contamination on the integrity of cement-formation interface. J Energy Res Technol.– 136(4): 2014.– P. 042908–042908.

https://doi.org/10.29013/AJT-22-7.8-16-21

Raupov A. A.,
PhD, Associate Professor,
Tashkent State Technical University
Murtazaev A. M.,
Candidate of technical sciences, Professor,
Tashkent State Technical University
Sokhibov D. Z.,
Basic doctoral student,
Tashkent State Technical University

DRILLING MIXES TO CREATE NEW COMPOSITIONS AND RESEARCH PROPERTIES

Abstract. In the article, the structure of modified starch obtained in different proportions was studied by means of IR-spectroscopy, SEM analysis, and its physical and chemical properties were analyzed. The resulting modified starch, which forms the basis of new compositions, allows the use of drilling mixtures at different pressures and temperatures in oil and gas wells.

Keywords: phosphorus, mineral powder (calcium carbonate), modified starch, IR-spectroscopy, electron microscope analysis, drilling mixtures.

Introduction. Today, the production of modified starch is increasing year by year worldwide. In 2016–2017 alone, production was expected to reach 9.36 billion US dollars, and according to experts, it is predicted to grow by 5.7% by 2025. In the global market for the production and consumption of modified starch, the leading countries such as the USA, China, Europe and Russia have achieved large production and are widely used in food, pharmaceutical, oil and gas well drilling [1].

Exploration of hydrocarbon products and drilling in high temperature and pressure conditions are becoming more difficult. This situation can be attributed to the decrease of reserves of oil and gas products, changes in pressure and temperature during drilling, inefficiency of the rheological properties of the drilling fluids, pollution of the interstices of the underground layer or deterioration of the geological parameters of the rocks, deterioration of the pipelines, changes in the shale layers and high technological pressure. complicated the processes. In order to overcome these problems, the fact that, as a result of the use of modified starch-based drilling fluids, has properties such as pressure, normalization of aquifers, and control of the mixture density, there is an opportunity for scientific research and the development of effective technologies in this field [2; 3; 4].

Some properties of modified starch, such as molar mass, chemical structure, and solubility, as well as their effects on reservoir corrosion and oil refining efficiency, are widely studied by researchers [5; 6]. Based on research on the modification of starch derivatives obtained from various raw materials, several methods of synthesis have been developed, the result of the analysis of the optimal conditions of the reaction, the degree of modification and the physico-chemical properties of the derivatives are being studied [7; 8].

In order to obtain and widely use the modified starch offered by us in drilling, which is necessary

in the production of local raw materials – the starch contained in rice husks, the production enterprises of «Uzkimyosanoat» JSC focus on the preparation of mixtures consisting of compounds containing metal, phosphorus, and nitrogen.

Polymer composite mixtures widely used in drilling oil and gas wells have high stabilization properties, they form a dispersed system in cold water and provide an opportunity to control moisture during the drilling process. In the implementation of these goals, it is possible to obtain modified starches with the help of a reactor under the influence of temperature with dehydrated starch products, ammonium polyphosphate and mineral powder (calcium carbonate) reagents.

Starch, ammonium polyphosphate and mineral powder (calcium carbonate) (3:0.5:1), (3:2:2), (2:2:2) and (3:1:1) reagents were prepared using a reactor under the influence of temperature. MKPM brand modified starch was obtained in different proportions and their proportions are as follows:

Starch	100–150
Ammonium polyphosphate	10–15
Mineral powder (calcium carbonate)	30–50

Table 1.– Properties of modified phosphorus-retaining malleable starch composites

MKPM modified starch	proportions	Properties of the drilling mixture				
		Conditional viscoelasticity	rotational viscometer rotation speed, rpm			water loss, cm^3/30 min
			600	300	3	
Starch, ammonium polyphosphate and mineral powder (calcium carbonate)	3:0,5:1	39	148	137	280	7
	3:2:2	44	146	133	274	6
	2:2:2	45	133	124	241	5
	3:1:1	41	149	135	276	6

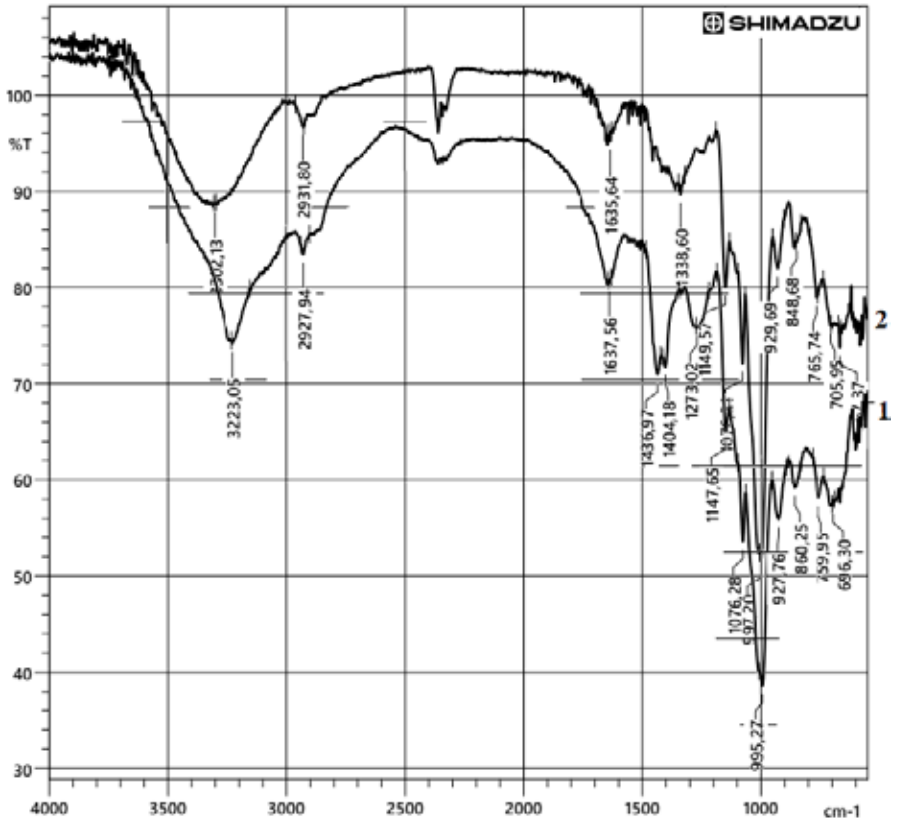

Figure 1. IK spectrum: 1 – starch; 2 – modified phosphorus-containing starch

In the course of research, changes in characteristic bonds were analyzed by IR spectroscopy of MKPM (starch, ammonium polyphosphate and mineral powder) brand modified starch. Accordingly, IR spectroscopy was performed using a Varian 3100 FT-IR spectrometer with a sampling range of 4000–400 cm^{-1}. The IR spectra show that when the IR spectra of the modified starch etherification products we offer are compared with unmodified starch (Fig. 1), new absorption lines appear: R––O groups at 504 cm^{-1} deformation vibrations, R–ON at 936 cm^{-1} – valence vibrations groups, 1718 cm^{-1} asymmetric valence vibrations – C=O carbamate groups and 1190 cm^{-1} – R=O groups. (Figure 1). 1019 cm^{-1} in the absorption range, characteristic of the IR spectrum characterizing the original starch, it can be shifted to the high frequency region up to 1024 cm^{-1} with a simultaneous increase in its intensity.

The formation of a composite structure, morphological changes of processes, and mixing of substances with each other have been studied through scanning electron microscope SEM analysis of modified phosphorus-containing starch. In these studies, modified starch particles ranging in size from 10 μm to 100 μm were investigated. It was investigated that the composition of the composites formed irregularly shaped granules with a polygonal shape. In addition, in the samples presented in the pictures, the composites obtained on the basis of different proportions of starch, ammonium polyphosphate and mineral powder (calcium carbonate) chemical reagents were studied (a) (2:2:2); (b) (3:0.5:1); (c) (3:2:2), and (d) (3:1:1) modified starch composite samples obtained on the basis of the ratios (b) and (d) in these ratios have the feature of a completely smooth surface (c) and (a) it is possible to analyze whether it formed a good mixture compared to composites. (Figure 2).

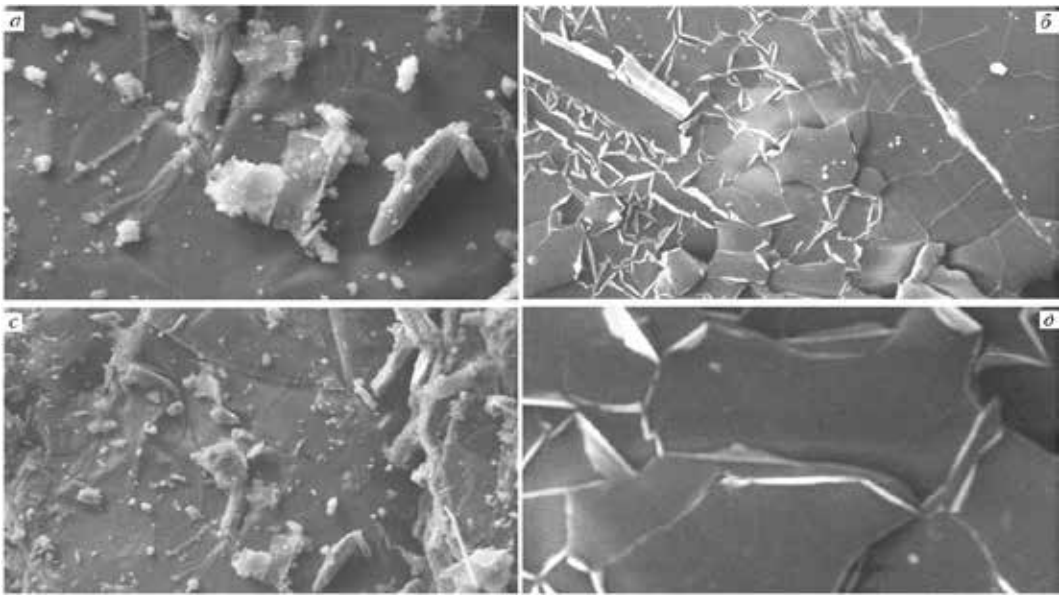

Figure 2. SEM Analysis: Starch, Ammonium Polyphosphate and Mineral Powder (Calcium Carbonate) Chemical Reagent Ratios; (2:2:2); (b) (3:0.5:1); (c) (3:2:2), and (d) (3:1:1)

(b) In this paper, the extraction process of carboxymethyl starch is also researched, this starch has the properties of forming a sticky paste in cold water, and the extraction process consists of simple technology. This modified starch is one of the economically and ecologically effective products that are stable to heat and biological effects. Carboxymethyl starch was obtained as a result of the reaction of etherification of hydroxyl groups with monochlorous acid or its sodium salts in an alkaline environment. In the first stage of the reaction, an equal amount of NaOH reacts with the hydroxyl groups of starch.

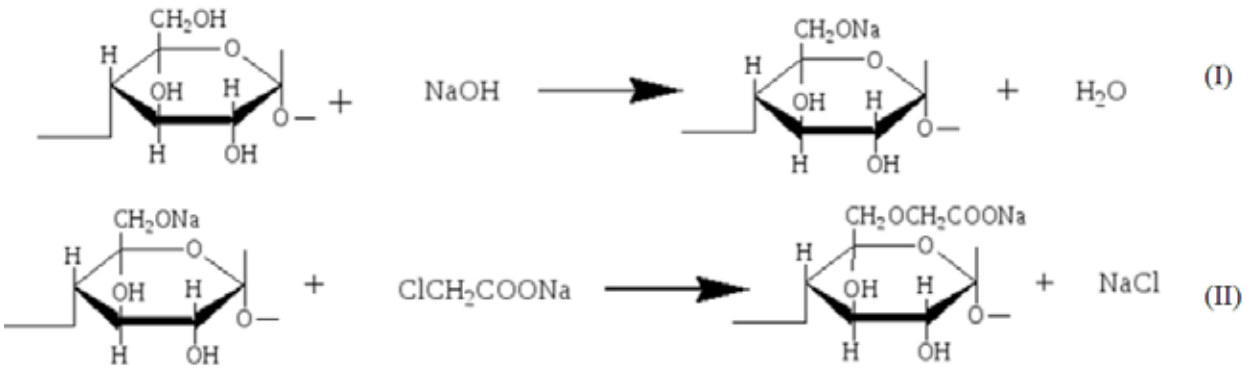

Figure 2.7. Reaction of carboxymethyl starch sodium salt

In the second step, the reaction process continues by replacing sodium monochloroacetate with a carboxymethyl group.

KMK-Na (sodium – carboxymethylstarch) are biopolymers with a high level of viscoelasticity, which can be analyzed with characteristic frequencies under IR spectroscopy.

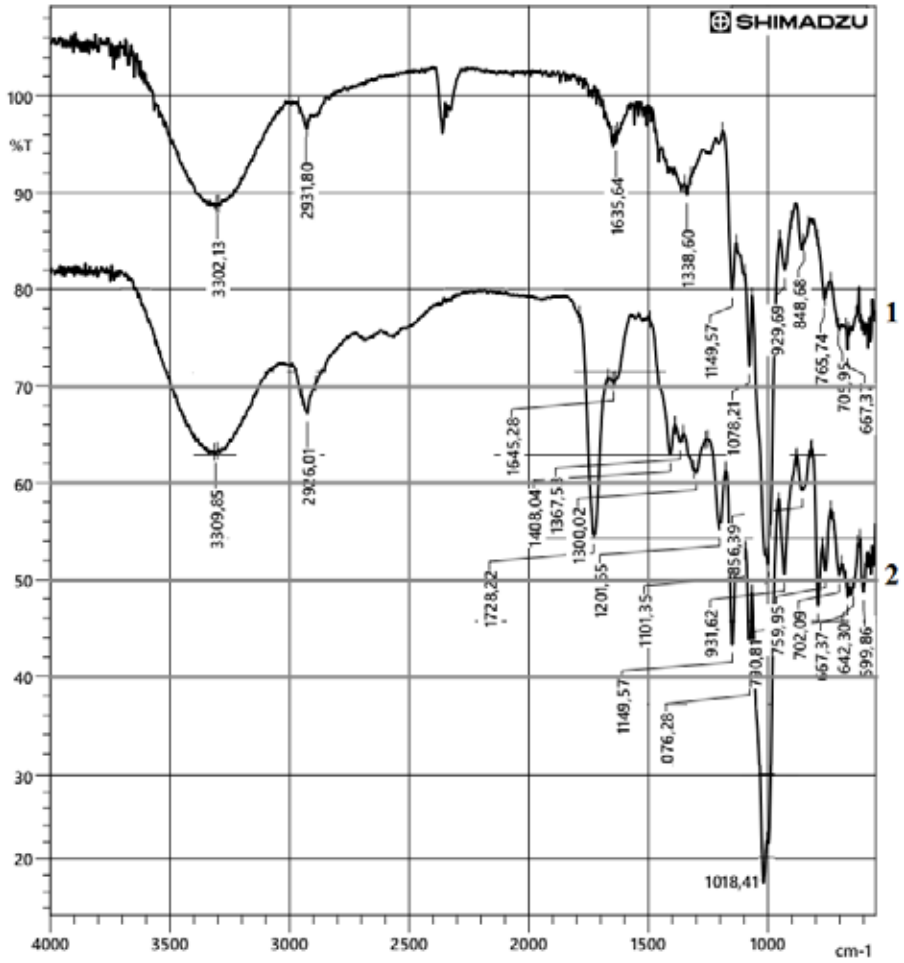

Figure 3. IK spectrum starch (1) and modified starch (2)

Figure 3 shows the IR spectroscopy of starch, and mainly hydroxyl groups have peaks in the region of 3365 cm^{-1}. In addition, frequencies related to the S-N group were observed in the range of

2950–2900 cm^{-1}. It can be seen that the frequency in the region of 1100–1000 cm^{-1} is characteristic of the SN2-O-SN2 group, showing valence and valence strains. IR spectroscopy of sodium carboxymethyl-starch and starch revealed frequencies in several different regions. According to it, it was studied that the hydroxyl group in the region of 3300 cm^{-1} and two new peaks at 1600–1400 cm^{-1} belong to the SOO-group in sodium carboxymethyl starch. There is also an absorption band at 1750–1700 cm^{-1} corresponding to the vibrations of the carboxyl group.

In addition, the physico-chemical properties of polyelectrolyte solutions differ from other types (in the case of electrolyte) of polymers. In polyelectrolytes, the formation of ionic bonds in the polymer structure greatly affects the viscosity of the solution, regardless of whether the solution is concentrated or diluted. In this process, the ionization structure causes a significant change in the conformation of the polymer in solution.

As a result, the viscous flow of polymers deviates from the straight line depending on the concentration of the solution ud/s = f(s). Figure 4 shows the dependence of the decrease in the viscosity of aqueous solutions of the sodium salt of carboxymethyl starch on the polymer concentration. It can be analyzed that this feature is characteristic of polyelectrolytes and differs sharply from starch.

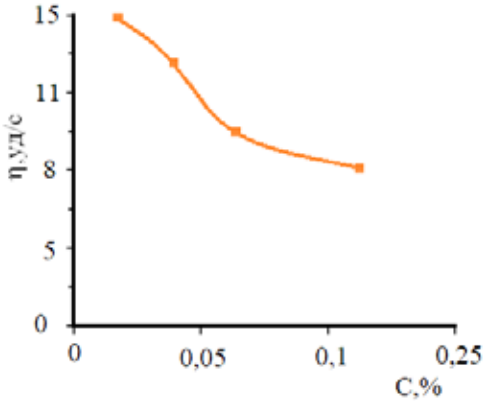

Figure 4. Dependence of the concentration of the viscosity of aqueous solutionsof the sodium salt of carboxymethyl starch

Carboxymethyl starch-based drilling compounds allow the use of various temperatures in oil and gas wells. Drilling mixtures containing carboxymethyl starch (KMK) are stable to mineralization and temperature, and their proportions are based on their composition, mass.%.

Carboxymethyl starch (KMK)	3.0–3.5
Sodium hydroxide	0.02–0.03
Sodium carbonate	0.02–0.05
Sodium chloride	30–33
mineral powder (calcium carbonate)	10–12
copolymer based on acrylic starch	1–2
bentonite	7–10
water is normal	

The properties and characteristics of the proposed drilling mix are studied and the results are presented in (Table 2).

Table 2. – Properties of drilling compound based on carboxymethyl starch (KMK)

№ т/р	The name of Indicators	Unground mixture	Ground mixture
1	appearance	powder	powder
2	colour	Pale yellow	Pale yellow
3	the smell	odorless	odorless
4	density	10.8	10.8
5	environment, pH	7.5–8.0	7.5–8.0
6	solubility, 22°C	soluble in water	

Thus, chemical reagents based on starch, ammonium polyphosphate and mineral powder (calcium carbonate) (3:0.5:1), (3:2:2), (2:2:2) and (3:1:1) Mineralization of drilling mixtures containing MKPM modified starch and carboxymethyl starch (KMK) with the help of ammonium polyphosphate and mineral powder (calcium carbonate) under the influence of temperature using a reactor allows creat-

ing new compositions of temperature-stable drilling mixtures.

In conclusion, we can say that the current process of globalization is affecting the oil and gas industry as well as other industries. Therefore, it is one of the most important problems to study and analyze the chemical components and reagents used in oil and gas wells. As a result of studies, the concentration dependence of the viscosity of aqueous solutions of mineralized drilling mixtures with the help of modified MKPM and KMK ammonium polyphosphate and mineral powder (calcium carbonate) makes it possible to use them in oil and gas wells at different temperatures.

References:

1. Modified Starch Market Size, Share & Trends Analysis Report By Product (Starch Esters & Ethers, Resistant, Cationic), By Material, By Function, By End Use (F&B, Animal Feed, Paper, Textiles), And Segment Forecasts, 2019.– 2025. URL: https://www.grandviewresearch.com/industry-analysis/modified-starch-market
2. Al-Muntasheri G., Nasr-El-Din H., Hussein I. A rheological investigation of a high temperature organic gel used for water shut-off treatments. J Pet Sci Eng.– 59(1–2): 2007.– P. 73–83.
3. Olivia V. López, Luciana A. Castillo, Mario D. Ninago, Andrés E. Ciolino, and Marcelo A. Villar. Modified Starches Used as Additives in Enhanced Oil Recovery (EOR) // See discussions, stats, and author profiles for this publication at: URL: https://www.researchgate.net/publication/319083538 Chapter. August 2017.– P. 227–233. DOI: 10.1007/978–3–319–61288–1_9
4. Aboulrous A. A., Alsabagh A. M., Abdou M. I., Khalil A. A., Ahmed H. E. Investigation of some locally water-soluble natural polymers as circulation loss control agents during oil fields drilling. Egypt J of Petr.– 23(1): 2014.– P. 27–34. URL: https://doi.org/10.1016/j.ejpe.2014.02.005.
5. Manal A. E. Carboxymethylation of maize starch at mild conditions. CarbohydrPolym.– 79(4): 2010.– P. 875–881. URL: https://doi.org/10.1016/j.carbpol.2009.10.013.
6. Aliyu Adebayo Sulaimon. Evaluation of drilling muds enhanced with modified starch for HPHT well applications // Received: 23 July 2019 / Accepted: 17 October 2020. Journal of Petroleum Exploration and Production Technology. URL: https://doi.org/10.1007/s13202–020–01026–9
7. Ghazali N. A., Alias N. H., Mohd T. A.T., Adeib S. I., Noorsuhana M. Y. Potential of corn starch as fluid loss control agent in drilling mud. Appl. Mech. Mater. 2015.– P. 754–755, 682–687.
8. Soto D., Urdaneta J., Pernía K., León O., Muñoz-Bonilla A., Fernandez-García M. Removal of heavy metal ions in water by starch esters.– Starch-Starke – 68. 2016.– P. 37–46.

Section 2. Transport

https://doi.org/10.29013/AJT-22-7.8-22-25

Suleimanova Kamila,
Master in Traffic Information Engineering and Control,
The Faculty of Automation
Nanjing University of science and technology

DEVELOPMENT OF AUTOMATED TRAFFIC CONTROL SYSTEMS USING ARTIFICIAL INTELLIGENCE

Abstract. Almost all major cities suffer from significant traffic congestion. To achieve improved detection performance and multi-vehicle recognition in a complex urban environment, a detection algorithm based on histogram oriented gradients (HOG) features is applied. This algorithm takes full advantage of HOG for vehicles, i.e. we can talk about the good descriptive ability of the HOG function. With ever-increasing demand for urban mobility and modern developments in logistics, the number of vehicles has been steadily increasing over the past few decades.

In our proposed method, the system is designed to control the time of a traffic light depending on the traffic density on the corresponding road. It acts as a multi-class classification that recognizes traffic. The system detects a traffic event in real time.

Keywords: capacity, multiclass classification, automated traffic control system, planning algorithm, traffic intensity.

With the ever-increasing demand for urban mobility and the expansion of the modern logistics sector, the vehicle fleet has grown steadily over the past few decades. One of the natural consequences of the growth of the vehicle fleet is the increase in traffic congestion. The normal operation of a traffic light requires supervision and coordination to ensure that vehicles and pedestrians move smoothly and as safely as possible. For this, a variety of control systems are used, ranging from simple clockwork to complex computerized control and coordination systems that self-adjust to minimize the delay of people using the intersection.

According to the international classification, four generations of systems should be distinguished that allow managing traffic [1, p. 24]:

1. First generation systems, in which all calculations necessary for traffic coordination were performed manually.

2. Second generation systems, within the framework of which partial automation of the traffic control process on the roads was carried out.

3. Third-generation systems, which made it possible to fully automate the control process based on predictive data on the degree of traffic congestion.

4. Fourth generation systems that allow traffic management based on real-time traffic data.

Currently, all existing traffic control systems can be divided into three main categories:

1. Systems of decentralized type.

2. Systems of a centralized type.

3. Intelligent type systems.

As part of the use of decentralized traffic control systems on the roads, there is no need for the system to be connected to a single control center.

When using centralized traffic control systems, on the contrary, all data falls into a single control center that coordinates the entire work process.

Intelligent systems are similar to centralized ones, as all traffic data goes to a single center. The difference lies in the fact that in simple centralized systems decisions are made by personnel, and in intelligent systems – by a computer using artificial intelligence technologies.

Accordingly, the most advanced, and therefore most often used in large cities, are intelligent systems, one of the variants of which will be proposed in this scientific article.

These innovative software projects provide an effective means of understanding traffic scenarios that allows you to control a 4-way traffic signal control system. The system consists of 4 signals corresponding to each road. In this paper, we propose planning traffic signals based on a density algorithm. The system is designed to control the timing of traffic lights depending on the traffic density on the corresponding road. The system presents road congestion traffic graphically using traffic signaling devices. Measuring traffic on a particular road gives you the ability to adjust signal timings to allow that particular path to clear and then move on to the next problem area. The whole system works according to an algorithm that allows you to smoothly and effectively regulate the traffic flow in all four directions. It also includes an emergency stop system that allows control operators to remotely turn off a particular signal in the event that an ambulance or an important vehicle is following the path.

Many researchers have studied various types and techniques of multi-traffic scene perception and also in the field of social networks, since it is useful in terms of basic multi-traffic scene perception for vehicle detection. Scientists from India, in particular, are focused on the analysis and implementation of the twitter feed with real-time traffic detection and the search for a framework that allows you to check the event and identify the location of activity through the study of the twitter feed.

Italian expert Alberto Rosi has studied social sensors and pervasive approaches to services and the perspectives they provide, as this social perception technique is integrated into the computing system.

Chinese experts studied the multi-vehicle detection algorithm by combining the functions of Harr and HOG, based on which they developed a system to achieve better performance for multi-vehicle detection in complex urban environments. environment with a two-stage detection algorithm. This system provides higher vehicle detection accuracy and is also more time efficient.

Indian scientists were implementing a project to develop an automatic traffic light system for the city of Chandigarh. This is a system monitoring that allows you to automatically identify the traffic flow in the signal traffic. This system also had sensors that sense road data in traffic. This system provided real-time traffic detection and eliminated the loss of green light time needed to optimize traffic on the relevant section of the road.

Chinese scientists have also explored automatic environmental recognition changes for drivers in the driver assistance system. They developed a computational model to study critical environmental changes for drivers in a driver assistance system. They demonstrated the practicality of a computational model for recognizing changes in the system under study.

Chinese scientists have also improved the vehicle detection method based on the Bio-Inspired approach to improve the image by the feature fusion method of the weighted evaluation level. Using this method of vehicle detection was possible even at night. Thanks to this system, it was possible to deal with a significant number of different types of scenes, including cars of different types and sizes. It also allowed identification of a vehicle in various locations and vehicle numbers.

Japanese experts studied the possibility of vehicle detection using active learning and derivative symmetry analysis. They developed a system that worked on the road to detect the vehicle, which was a very important operation. This system uses seven types of data sets to track road, weather, and traffic conditions.

French specialists have developed a multidimensional model for classifying high-resolution optical images based on wavelets of texture features. This model was based on the strategy of a supervised classification system that classified images according to a training database storing information to enable the classifier to make a decision.

Convolutional Neural Network (CNN) is one of the most popular deep learning algorithms. CNNs are used to recognize and classify images and videos. In our system, we use this algorithm to calculate traffic density. At each stage, feature extraction is performed, and it produces a large set of features for the original input. These feature sets help describe the characteristics of the data. Each frame is classified and the resulting value is displayed in the video frame window.

To detect vehicles, the Hoard backlight descriptor is used, which defines a picture on a 64x128 fix. Obviously, the image can be any size. Usually corrections at different scales are checked on many areas of the image. The main limitation is that kink patches have a fixed angular proportion. For our situation, the patches should have a 1:2 aspect ratio. For example, they may be 100 × 200, 128 × 256, or 1000 × × 2000, but not 101 × 205.

To calculate the HOG descriptor, we initialize the calculation of the horizontal and vertical gradients; then the histogram of the gradients should be calculated. This makes it possible to simply filter the image using subsequent procedures.

At this stage, the image is divided into 8 × 8 cells and the band of the gradient graph is calculated for each 8 × 8 cells.

The gradient of the picture is very sensitive to the level of general lighting. In case you make the image darker by dividing all the pixel values by 2, the value of the tilt angle will change significantly, and together these lines of the evaluation histogram will change very significantly. In an ideal world, we want our handle to be free of lighting options. Thus, there is a need to "standardize" the histogram so that it is not affected by lighting variations.

To compute the last element vector for the entire fix image, the 36 × 1 vectors are concatenated into one giant vector. What is the size of this vector? Let us calculate.

1. How many places do we have in 16 × 16 squares? There are 7 levels and 15 vertical positions in total. 7 × × 15 = 105 positions.

2. Each 16x16 square is checked against a 36×1 vector. Therefore, when we connect them all into one giant vector, we get a dimension of 36 × 105 = 3780 vectors.

The current location of the traffic light gives a fixed traffic control plan, the settings of which depend on the previous ones. However, traffic checks can be physically modified. This is the most widely recognized type of sign control for day-to-day management and can cause the system to misbehave at an hour that is different from what the layout was based on, such as utilizing redundant stages when there is little traffic.

We can integrate our system with official traffic signal analysis app to capture real-time status notification traffic. Thus, our system will be able to signal traffic-related events even in the worst case.

In addition, we are exploring the possibilities of integrating our system into a more sophisticated traffic detection infrastructure. This infrastructure can include both advanced physical sensors and social sensors such as social media streams. In particular, social sensors can provide low cost wide coverage of the road network, especially in areas (urban and suburban) where traditional traffic sensors are not available.

Thus, the control system considered in the paper has significant advantages in organizing traffic on the roads and optimizing it, which is achieved, first of all, by using elements of artificial intelligence in it.

The system allows:

1. Introduce an integrated approach to the organization of the traffic system in large cities.

2. Actively apply visual traffic control with vehicle type recognition.

3. Significantly save money in large cities by reducing losses that inevitably arise as a result of vehicles standing idle in traffic jams.

References:

1. Elanskaya M. V., Lyubichev D. M., Dormidontova T. V. Automated traffic control system // Eurasian Union of Scientists (ESU).– No. 4. 2019.– P. 22–25.
2. Litvinenko N. A. Review of modern technical means of traffic organization in the Russian Federation // European science.– No. 1. 2017.– P. 13–14.
3. Porubov D. M., Beresnev P. O., Tyugin D. Yu. The system of automated control of the movement of vehicles based on the recognition of the road scene and its objects // Izvestiya MSTU "MAMI".– No. 1. 2018.– P. 52–63.

Section 3. Physics

https://doi.org/10.29013/AJT-22-7.8-26-30

Rasulov Voxob Rustamovich,
PhD, associate professor of Fergana State University
Rasulov Rustam Yavkachovich,
Professor of Fergana State University
Farmonov Islam Elmar-ugli,
Master of Fergana State University
Holmatova G. M.,
Master of Fergana State University

DIMENSIONALLY QUANTIZATION OF THE ENERGY SPECTRUM OF HOLES IN A P-Te QUANTUM WELL

Absract. The dimensionally quantization in a potential well grown on the basis of a gyrotropic crystal (for example, p-Se or p-Te) is theoretically investigated.

Expressions are obtained for the wave functions of holes depending on the dimensionally quantization number.

It was shown that the dimensionally-quantized spectrum of holes in gyrotropic crystals depends on the ratio of the hole energy to the height of the potential barrier. In particular, the energy spectrum of holes in the well consists of a set of dimensionally-quantized levels that do not intersect with each other due to the presence of an energy gap between subbands of the valence band.

Keywords: dimensionally quantization, wave function, holes, energy spectrum.

I. Introduction

Recently, considerable attention has been drawn to dimensionally quantization (DQ), which has applications in optoelectronics [1]. For semiconductors with a simple band structure, the study of interlevel optical transitions in structures for an arbitrary potential was carried out in [2; 3]. At the same time, interlevel optical transitions in semiconductor structures with hole conductivity are of interest because of the nonzero absorption for light of arbitrary polarization, which have practical applications [4]. A theoretical study of this kind of problem is hampered by the complexity of the band structure of the crystal.

In particular, in [5–7], such a problem in the case of a rectangular dimensionally quantized well (DQW) with a fixed thickness was solved numerically. However, even a small variation in the thickness or depth of the RQW can greatly change the final result, which makes it difficult to analyze intermediate calculations. In [8], on the basis of perturbation theory, analytical expressions [9] were obtained; the energy spectrum, the wave function of holes, and the intersubband absorption of polarized radiation

in an infinitely deep quantum well of a semiconductor were studied. The calculations were carried out in the Luttinger-Kohn approximation [10; 11] for semiconductors with a zinc blende lattice.

However, the theoretical study of dimensional quantization in a potential well (DQW) grown on the basis of a gyrotropic crystal (for example, *p-Se* or *p-Te*) remains open, which is the subject of this communication.

Note that the study of a number of phenomena, in particular, optical or photovoltaic effects in dimensionally-quantized structures (QW) requires knowledge of the energy spectrum and wave functions of electron current carriers.

II. Basic ratios

For a quantum well with a potential $U(z)$, the effective Hamiltonian for a quantum well with a potential $U(z)$ is the effective Hamiltonian of electrons in *p-Te* in the form

$$\widehat{H} = \widehat{H}_0 + \sum_{\alpha=x,z} A_\alpha \sigma_\alpha , \qquad (1)$$

where $\widehat{H}_0 = Ak_\perp^2 + Bk_z^2$, $A_x = \Delta$, $A_z = \beta k_z$ and it is assumed that the phases of t $M_{1,2}^{'}$ he function are chosen so that the coefficient at k_z is real, 2Δ – spin-orbit splitting of the valence band at the M(P) point of the Brillouin zone), $k_\perp^2 = k_x^2 + k_y^2$, A, B, β_V are band parameters of *p-Te*, $\vec{k}_\perp = k_\perp(\sin\varphi, \cos\varphi)$ is two-dimensional wave vector directed along the interface.

The wave functions in the upper valence bands (M'_1 and M'_2) are a superposition of states with the projection of the angular momentum on the axis Z $(m_z = \pm 3/2)$

$$\Psi_{M'_1} = \sum_{m_z=\pm 3/2} C_{m_z}^{(l)} \mid m_z \rangle , \qquad (2)$$

where $C_{3/2}^{(1)} = C_{-3/2}^{(2)} = C_1 = \sqrt{(1+\eta)/2}$, $C_{-3/2}^{(1)} = -C_{3/2}^{(2)} = = C_2 = \sqrt{(1-\eta)/2}$, $\eta = \beta k_z (\Delta^2 + \beta^2 k_z^2)^{-1/2}$.

The spectrum of holes in the valence band in a bulk gyrotropic crystal has the form

$$E_l(k_x, k_y, k_z) = Ak_\perp^2 + Bk_z^2 - (-1)^{-l}\left(\Delta^2 + \beta^2 k_z^2\right)^{1/2} \quad (l = 1,2). \qquad (2')$$

Here $A = \hbar^2/(2m_\perp), B = \hbar^2/(2m_{||})$, $m_\perp$ and $m_{||}$ are the transverse and longitudinal effective masses of holes in the subbands M'_1 and M'_2, which are equal with the opposite sign to the effective masses of electrons.

Then choosing the dimensionally quantization axis Oz and assuming that $k_z = \frac{1}{i}\frac{\partial}{\partial z}$ from (1) we have

$$\widehat{H} = \widehat{H}_0 + \widehat{R}_2 k_\perp^2 , \qquad (3)$$

where

$$\widehat{H}_0 = \Delta\begin{bmatrix} 0 & 1 \\ 1 & 0 \end{bmatrix} - B\begin{bmatrix} 1 & 0 \\ 0 & 1 \end{bmatrix}\frac{\partial^2}{\partial z^2} - i\beta_V \begin{bmatrix} 1 & 0 \\ 0 & -1 \end{bmatrix}\frac{\partial}{\partial z} + U(z),$$

$$\widehat{R}_2 = A\begin{bmatrix} 1 & 0 \\ 0 & 1 \end{bmatrix}k_\perp^2 , \qquad (4)$$

III. Hole states in a tellurium quantum well

The unperturbed energy levels $E_\xi(0)$ and the wave function of electrons $\psi_\xi^{(0)} = \begin{bmatrix} \psi_2^{(0)} \\ \psi_1^{(0)} \end{bmatrix}$ in the subbands M'_ξ $(\xi = 2,1)$ the conduction band of $p-Te$ are determined from the following matrix differential equation with band parameters A, B:

$$\widehat{H}_0 \bar{\psi}_\xi^{(0)} = \widehat{E}_\xi \bar{\psi}_\xi^{(0)} , \qquad (5)$$

where $\widehat{E}_\xi = \begin{bmatrix} \tilde{E} & 0 \\ 0 & \tilde{E} \end{bmatrix}$. Then we have

$$\left\{\frac{\Delta}{2}\begin{bmatrix} \psi_2^{(0)} \\ -\psi_1^{(0)} \end{bmatrix} - \frac{\partial^2}{\partial z^2}\begin{bmatrix} A_3\psi_2^{(0)} \\ A_1\psi_1^{(0)} \end{bmatrix} + U(z)\begin{bmatrix} \psi_2^{(0)} \\ \psi_1^{(0)} \end{bmatrix}\right\} = = \begin{bmatrix} \tilde{E}\psi_2^{(0)} \\ \tilde{E}\psi_1^{(0)} \end{bmatrix}, \qquad (6)$$

To simplify the problem, we assume that $U(z) = U_0 = const$. Then the last equation will look like

$$\begin{cases} \dfrac{\partial^2\psi_2^{(0)}}{\partial z^2} - \dfrac{1}{B}\left[U(z) - \tilde{E}\right]\psi_2^{(0)} + i\dfrac{\beta_V}{B}\dfrac{\partial\psi_2^{(0)}}{\partial z} - \dfrac{\Delta}{B}\psi_1^{(0)} = 0, \\ \dfrac{\partial^2\psi_1^{(0)}}{\partial z^2} - \dfrac{1}{B}\left[U(z) - \tilde{E}\right]\psi_1^{(0)} - i\dfrac{\beta_V}{B}\dfrac{\partial\psi_1^{(0)}}{\partial z} - \dfrac{\Delta}{B}\psi_2^{(0)} = 0 \end{cases} \qquad (7)$$

or

$$\frac{\partial^2\psi_+^{(0)}}{\partial z^2} - \kappa_E^2\psi_+^{(0)} + i\kappa_{\beta_V}\frac{\partial\psi_-^{(0)}}{\partial z} - i\kappa_\Delta^2\psi_-^{(0)} = 0, \qquad (8)$$

where $\kappa_E^2 = \frac{1}{B}\left(U_0 - \tilde{E}\right)$, $\kappa_\Delta^2 = \frac{\Delta}{B}$, $\kappa_{\beta_V} = \frac{\beta_V}{B}$, $\psi_\pm^{(0)} = \psi_2^{(0)} \pm i\psi_1^{(0)}$.

We will seek solution (8) in three approximations, which we analyze in more detail below.

1. Approximation. From (8) it is easy to obtain the following system of equations

$$\begin{cases} \dfrac{\partial^2 \psi_+^{(0)}}{\partial z^2} - \kappa_E^2 \psi_+^{(0)} = 0, \\ \dfrac{\partial \psi_-^{(0)}}{\partial z} + \dfrac{\kappa_\Delta^2}{\kappa_{\beta_V}} \psi_-^{(0)} = 0, \end{cases} \quad (9)$$

whose solution we write in the form

$$\psi_\pm^{(0)} = D_\pm \exp(\kappa_\pm z) + C_\pm \exp(-\kappa_\pm z), \quad (10)$$

where $\kappa_+ = \kappa_E$, $\kappa_- = \kappa_\Delta$, unknown quantities $D_\pm$, C_1 are determined from the boundary conditions of the problem, which will be discussed further. Note that κ_- the real value, κ_+ parameter can be both real (at $U_0 \rangle \tilde{E}$) and imaginary (at $U_0 \langle \tilde{E}$) values. Then the wave function $\psi_+^{(0)}$ in the first case will be exponential, and in the second case it will be trigonometric. If $\kappa_\pm$ the value is real, then we can assume that $D_\pm = 0$. This means that current carriers (holes in *p-Te*) with energy $\tilde{E} \langle U_0$ will behave like a de Broglie (plane wave), but in other cases they will not.

Further, we assume that the holes are in the potential well. Then

$$\psi_+^{(0)} = D_+ \exp(i\kappa z) + C_+ \exp(-i\kappa z),$$

$$\psi_-^{(0)} = C_1 \exp\left(-\frac{\kappa_\Delta^2}{\kappa_{\beta_V}} z\right), \quad (11)$$

where it is taken into account that $U_0 = 0$, $\kappa_+ = i\sqrt{\tilde{E}/B} = i\kappa$. Then, from the conditions of orthonormality and finiteness of the wave functions of holes at the interfaces of the well, we have that

$$\psi_+^{(0)}(z) = 2\kappa^{1/2} \frac{\cos(\kappa z)}{\left[2\kappa a + \sin(2\kappa a)\right]^{1/2}}. \quad (12)$$

From the boundary condition of the problem, we obtain expressions for the size-quantized energy spectrum of holes

$$\tilde{E} = B \frac{(2n+1)^2}{4a^2} \pi^2 \quad (n = 0,1,2,...) \quad (13)$$

2. Approximation. Now we look for the solution of equation (8) in the form

$$\psi_+^{(0)} = D \exp(\kappa z) \quad \psi_-^{(0)} = D^* \exp(\kappa^* z), \quad (14)$$

where κ^* and D^* are the complex conjugate wave vector and a parameter whose analytical form can be determined from the above boundary conditions. Then it is easy to obtain the following relations, useful for further calculations

$$D_{im} = i \cdot \frac{\left[\left(-\kappa^2 + \kappa_E^2\right) + i\left(-\kappa^* \kappa_{\beta_V} + \kappa_\Delta^2\right)\right]^2}{\left(-\kappa^2 + \kappa_E^2\right)^2 + \left(-\kappa^* \kappa_{\beta_V} + \kappa_\Delta^2\right)^2} D_{re}, \quad (15)$$

where D_{re} and D_{im} are the real and imaginary values of the quantity. It can be seen from (15) that the form of the wave function (14) depends on the physical nature of the wave vector. Therefore, consider the following cases:

a) let the wave vector be a real value, then

$$D_{im} = -2 \frac{\varsigma_{re}}{\varsigma_{re}^{\ 2} + 1} D_{re}, \quad (16)$$

where $\varsigma_{re} = \left(-\kappa^2 + \kappa_E^2\right) / \left(-\kappa \kappa_{\beta_V} + \kappa_\Delta^2\right)$. Then the wave functions of holes take the form

$$\psi_\pm^{(0)}(z) = \frac{\varsigma_{re}^{\ 2} + 1 \mp 2i\varsigma_{re}}{\varsigma_{re}^{\ 2} + 1} D_{re} \exp(\kappa z). \quad (17)$$

Then the energy spectrum of current carriers is determined from the following transcendental equation

$$\left(\frac{\tilde{E}}{B}\right)_\pm = \frac{\varsigma_{re}}{\varsigma_{re}^{\ 2} + 1} \kappa_{\beta_V} \pm$$

$$\pm \left[\left(\frac{\varsigma_{re}}{\varsigma_{re}^{\ 2} + 1} \kappa_{\beta_V}\right)^2 + 4\left(\frac{\tilde{E}^2}{B^2} - \frac{2\varsigma_{re}}{\varsigma_{re}^{\ 2} + 1} \kappa_\Delta^2\right)\right]^{1/2}. \quad (18)$$

It can be seen from (18) that the energy spectrum takes real values when the following inequalities are fulfilled

$$\tilde{E} \rangle \frac{B}{2}\left[\frac{2\varsigma_{re}}{\varsigma_{re}^{\ 2} + 1} \kappa_\Delta^2 - \left(\frac{\varsigma_{re}}{\varsigma_{re}^{\ 2} + 1} \kappa_{\beta_V}\right)^2\right]^{1/2},$$

$$\frac{2\varsigma_{re}}{\varsigma_{re}^{\ 2} + 1} \kappa_\Delta^2 \rangle \left(\frac{\varsigma_{re}}{\varsigma_{re}^{\ 2} + 1} \kappa_{\beta_V}\right)^2; \quad (19)$$

b) let the wave vector be an imaginary quantity, then the relationship between the quantities D_{im} and D_{re} is described as

$$D_{im} = -2 \frac{\varsigma_{im}}{\varsigma_{im}^2 + 1} D_{re}, \quad (20)$$

and the wave functions of holes are determined by

$$\psi_+^{(0)}(z)=\frac{2D_{re}}{1+b_2^2}(1+ib_2)\exp(\kappa z),$$

$$\psi_-^{(0)}(z)=D_{re}\left(1-\frac{(1+ib_2)^2}{b_2^2}\right)\exp(\kappa z), \quad (21)$$

where $\varsigma_{im}=\left(\kappa^2+\kappa_E^2-\kappa\kappa_{\beta_V}\right)/\kappa_\Delta^2$. $b_2=\dfrac{\kappa_\Delta^2-\kappa^*\kappa_{\beta_V}}{\kappa_E^2-\kappa^2}$.

Now let's try to solve the system of equations (7) in general form. To do this, after transforming in (7), it is easy to obtain the Schrödenger equation in the form

$$\frac{\partial^4\psi_2^{(0)}}{\partial z^4}-\frac{1}{B}\left(U_0-\tilde{E}-\frac{\beta_V^2}{B}\right)\frac{\partial^2\psi_2^{(0)}}{\partial z^2}-$$

$$-\frac{1}{B^2}\left\{\Delta^2-\left(U_0-\tilde{E}\right)^2\right\}\psi_2^{(0)}=0. \quad (22)$$

Consider the following cases:

a) for holes located in the well $(U_0=0)$, equation (22) takes the form

$$\frac{\partial^4\psi_2^{(0)}}{\partial z^4}+\aleph_1^2\frac{\partial^2\psi_2^{(0)}}{\partial z^2}-\aleph_0^4\psi_2^{(0)}=0, \quad (23)$$

whose solution we seek in the form

$$\psi_2^{(0)}=B_2\cdot e^{-\alpha_1\cdot z}+B_2\cdot e^{\alpha_2\cdot z}+B_3\cdot e^{-\alpha_2\cdot z}, \quad (24)$$

where $\aleph_1^2=B^{-1}\left(\tilde{E}+B^{-1}\beta_V^2\right)$, $\aleph_0^4=B^{-2}\left(\Delta^2-\tilde{E}^2\right)$,

$\alpha_1=\aleph_-$, $\alpha_2=i\aleph_+$, $\aleph_\pm=\sqrt{\dfrac{1}{2}\left[\pm\left(\aleph_1^2\right)+\sqrt{\left(\aleph_1^2\right)^2+4\aleph_0^4}\right]}$

and, in what follows we will take into account that $\left(\aleph_1^2\right)\langle\sqrt{\left(\aleph_1^2\right)^2+4\aleph_0^4}$. Then, from the conditions of finiteness of the wave functions at the interface boundaries, we have

$$\psi_2^{(0)}(z)=\frac{B_2}{2}\left[\frac{e^{(2i\aleph_-+\aleph_+)a}-e^{-\aleph_+\cdot a}-2i\sin(\aleph_-\cdot a)}{ch(\aleph_+\cdot a)-\cos(\aleph_-\cdot a)}\cdot\left(e^{-\aleph_+\cdot z}-e^{-i\aleph_-\cdot z}\right)+2\left(e^{i\aleph_-\cdot z}-e^{-\aleph_+\cdot z}\right)\right]. \quad (25)$$

where B_2 is determined from the normalization condition of $\psi_2^{(0)}(z)$.

The energy spectrum of holes in a potential well is determined by the relation

$$\sin(\aleph_-\cdot a)-cos(\aleph_-\cdot a)+\frac{\aleph_-}{\aleph_+}exp(-\aleph_+\cdot a)=0. \quad (26)$$

b) for holes outside the well $(U_0\neq 0)$, the wave function of holes is determined by expression (25) and the energy spectrum by relation (26), but the following substitutions must be made: $\aleph_1\leftrightarrow\wp_1$, $\aleph_0\leftrightarrow\wp_0$, where $\wp_0^4=\dfrac{1}{B^2}\left\{\Delta^2-\left(U_0-\tilde{E}_2\right)^2\right\}$, $\wp_1^2=\dfrac{1}{B}\left(U_0-\tilde{E}-\dfrac{\beta_V^2}{B}\right)$;

c) in case of resonance, i.e. when the energy of holes is numerically equal to the height of the potential barrier, then the wave function of holes is determined by expression (25) and the energy spectrum by relation (26), but the following substitutions must be made: $\aleph_1^2\leftrightarrow\aleph_{01}$, $\aleph_0\leftrightarrow\aleph_{00}$, where $\aleph_{01}=\dfrac{\beta_V}{B}$, $\aleph_{00}^4=B^{-2}\left(\Delta^2-\tilde{E}^2\right)$

It can be seen from relation (22) that the wave function of holes in the potential well has two terms, one of which is exponentially decaying, and the rest are oscillating.

Conclusion

Thus, it was shown that the dimensionally-quantized spectrum of holes in gyrotropic crystals has a complex form and depends on the ratio of the hole energy to the potential barrier height. In particular, the energy spectrum of holes in the well consists of a set of dimensionally-quantized levels that do not intersect with each other due to the presence of an energy gap between the sus M_1' and M_2'.

Expressions are obtained for the wave functions and energy spectra of electrons for various cases, differing from each other in the relations for the characteristic wave vectors, which, in turn, depend on the band parameters of the semiconductor and on the energy gap between the subbands of the valence band of a gyrotropic crystal.

References:

1. Ivchenko E. L. Optical spectroscopy of semiconductor nanostructures // E. L. Ivchenko-Harrow (UK): Alpha Science, 2005.– 350 p. ISBN: 1–84265–150–1.
2. Vorobyov L. E., Ivchenko E. L., Firsov D. A., Shalygin V. A. Optical properties of nanostructures. S.-Pb. Nakau. 2001.– 192 p. (in Russian).
3. Petrov A. G., Shik A. Interlevel optical transitions in potential wells. Phys. Rev.– Vol. 48. 1993.– P. 11883–1187.
4. Rasulov V. R., Rasulov R. Ya., Eshboltaev I. M., Sultonov R. R. Dimensionally quantization in n-GaP. FTP.– Vol. 54. 1995.– P. 358–362. (in Russian).
5. Chang Y.-C. Saturation of intersubband transitions in p-type semiconductor quantum wells. Phys. Rev.– Vol. B39. 2020.– P. 12672–12677.
6. Rasulov R. Ya., Rasulov V. R., Eshboltaev I., Mamadalieva N. S. Absorption of linearly polarized radiation in a dimensionally quantized well. Uzbek Physics Journal: – Vol. 20.– No. 3. 2018.– P. 361–365.
7. Petrov A. G., Shik A. Absorption of light by holes in quantum wells. FTP.– Vol. 28. 1994.– P. 2185–2191. (in Russian).
8. Rasulov V. R., Rasulov P. Y., Eshboltaev I. M., & Sultonov R. R. Dimensionally Quantization in n-GaP. Semiconductors,– Vol. 54(4). 2020.– P. 429–432. URL: https://doi.org/10.1134/S1063782620040132
9. Golub L. E., Ivchenko E. L., Rasulov R. Ya. Absorption of light by holes in quantum wells. FTP.– Vol. 29. 1995.– P. 1093–1099. (in Russian).
10. Ivchenko E. L., Rasulov R. Ya. Symmetry and real band structure of semiconductors.– Tashkent. "Fan". 1989.– 126 p. (in Russian).

Section 4. Chemistry

https://doi.org/10.29013/AJT-22-7.8-31-35

Ibragimov A. A.,
Tojiyev R. R.,
Doctoral student of Fergana Polytechnic Institute

STUDYING THE PHYSICAL AND CHEMICAL PROPERTIES WHEN ADDING THE SOL OF STABILIZED FERTILIZERS

Abstract. The article defines the chemical composition of nitrogen-potassium fertilizers obtained by introducing ash into the melt of ammonium nitrate at mass ratios of ammonium nitrate: ash = 100: (3–25) and a temperature of 180 °C. The density and viscosity of the ammonium nitrate melt with the addition of ash in the temperature range 160–185 °C were also determined, and the strength of the granules was determined at the above ratios of ammonium nitrate: ash.

Keywords: ammonium nitrate, ash, melt, nitrogen-potassium fertilizer, density, viscosity, strength of granules

Introduction

From practical and scientific experience in the production of granulated ammonium nitrate (AN), it has been established that in order to ensure good physical properties of granulated AN, the moisture content in it should not exceed 0.2%. This concentration of water can be achieved in pre-evaporators purged with hot air. However, such a result is difficult. In this regard, various additives are used that bind free moisture, which can be divided into: 1) substances or reaction transformation products that dissolve well in water and simultaneously carry nutritional properties, capable of producing crystalline hydrates, 2) substances that adsorb moisture, but do not carry nutritional load. The latter is usually introduced directly into the AS melt before its granulation.

The first class of the category includes magnesium and calcium-containing additives: magnesite, brucite, dolomite, calcite, etc. [1–3]. At present, magnesia additive is used in many enterprises of the CIS countries [2]. The magnesia additive is recognized as the best additive that eliminates AC caking. To obtain this additive, caustic magnesite obtained by roasting natural magnesite is used. Under production conditions, caustic magnesite is decomposed by 35% HNO_3, while obtaining a 40% solution of $Mg(NO_3)_2$. Anhydrous magnesium nitrate binds free water remaining in the AS melt and binds to $Mg(NO_3)_2 \cdot 6H_2O$, which ensures the production of product granules with good physical and chemical properties.

At present, $Mg(OH)_2$ and MgO and methods for their preparation are covered in applied research work done in the field of powder technologies [1].

It was shown in [4] that magnesium nitrate increases the transition temperature IV → III from 32 to 55 °C and III→II from 84 to 90 °C. When the AS melt is cooled, the following transformations proceed sequentially: melt → I, I → II, and II → IV, respectively, at 167, 128, and 50 °C, bypassing phase III.

Water-binding additives can include hemihydrate and anhydrite of gypsum or phosphogypsum, capable of attaching 1.5 or 2 molecules of water to form a solid crystalline hydrate $CaSO_4 \cdot 2H_2O$ [5; 6]. The condition for the reliability of the action of solid additives requires a high degree of their dispersion, ensuring uniform distribution of saltpeter granules over the mass, maximum use of additives and a high rate of moisture absorption from the mother liquor. It is noted in [6] that a finely divided addition of gypsum or phosphogypsum should be introduced into the melt at about 5% before prilling on a granulation tower. Fertilizer with the addition of phosphogypsum with an N content of 24% (wt.) Has a hygroscopic point of 67%, while for pure AS (under the same conditions) this figure is 59.5%.

An important task at present is to reduce the level of potential hazard of ammonium nitrate. For this, research is underway to select highly effective additives that improve the strength of granules and increase the thermal stability of the fertilizer [6].

Objects and methods of research

In our work, we used sunflower sol of the Republic of Uzbekistan composition. Ammonium nitrate with the addition of sol, the strength of the granules of the products was determined on the device MIP-10–1 according to GOST 21560.2–82. The density of the melts was determined by the pycnometric method [7–9], and the viscosity was determined on a VPZh-2 viscometer with a diameter of 1.77 mm.

The experiments were carried out as follows. Granulated ammonium nitrate produced by JSC Fargonaazot (34.5% N) was melted in a metal reactor in a thermostat filled with glycerin. Phosphate raw materials were added to the AS melt at 180 °C with stirring in such an amount that the weight ratio of AS melt: Sol was equal to 100: (3–25). The temperature was maintained using a contact thermometer. The melt was kept for 20 min, after which it was poured into a granulator, which is a metal cup with a perforated bottom, the hole diameter in which was 1.2 mm. Pressure was created in the upper part of the glass using a pump, then the melt was sprayed from the sixth floor of the building onto a plastic film lying on the ground. Drops of the melt, falling from a height, solidified and turned into granules [10; 11].

In conditions of a large shortage of nitrogen-potassium fertilizers in our country, ash for the production of nitrogen-potassium fertilizers attracting the ash of Uzbekistan and the development of a technology for producing nitrogen-potassium fertilizers based on these ash are relevant. Until now, these ash is not used in the production of nitrogen-potassium fertilizers. The paper provides a general description of the evils of Uzbekistan and the possibility of their use as a potash raw material in the production of nitrogen-potassium fertilizers.

Based on the foregoing, in this paper we investigated the processes of obtaining nitrogen-potassium fertilizer based on ammonium nitrate melt with the addition of ash, the chemical composition of which is shown in Table 1.

Table 1. – Chemical properties of ash

The chemical composition of ash	K	Na	P	Ca	Si	Fe	Al	Mg	O	CI	S	C	W
A	12.4	2.8	3.4	15.7	10.0	1.1	1.4	4.6	36.4	2.5	1.6	–	8.1
Б	13.6	2.2	2.4	19.2	2.4	0.6	0.9	6.7	39.4	2.2	1.5	8.9	–
C	8.8	2.4	2.3	12.4	10.0	1.0	1.4	3.3	34.1	4.7	0.9	16.0	2.7

Results and its discussion

In this report, we present the results of determining the strength of ammonium nitrate granules obtained by adding ash at the above weight ratios AS: Sol. The strength of the granules is one of the

most important indicators characterizing the stabilized ammonium nitrate.

After that, the strength of the granules was measured. In this case, granules of nitrogen-phosphorus fertilizers were obtained, similar in appearance to granules of pure AS. The strength of the granules is 2–3 mm in size. Experimental data are given in (Table 2).

As can be seen from the tables, the more ash additives are added to the AS composition, the higher the strength of the granules. Thus, the addition of ash in the AS melt in the amount of 100 : 20 increases the strength of the granules from 5.52 MPa to a nitrogen content of 27.54%. And the strength of standard AS granules is only 2.91 MPa. This suggests that the introduction of a sol into the AS melt leads to a compaction of the granule structure and an increase in its crushing strength and abrasion, which ultimately has an effect on reducing the caking of the product during storage.

Table 2. – Strength of fertilizer granules obtained by introducing ammonium nitrate and sol into the melt

Mass ratio AS: Sol	N,%	K_2O,%	Granule strength		
			kg/granule	kgs/sm^2	MPa
Granule diameter 2–3 mm					
100: 3	33.44	0.17	1.51	28.81	2.91
100: 5	32.76	0.29	2.01	30.62	3.16
100: 8	31.62	0.38	2.51	38.61	3.86
100: 10	30.31	0.47	2.80	43.26	4.31
100: 12	29.83	0.68	3.11	49.90	4.91
100: 15	29.19	0.89	3.37	53.75	5.34
100: 18	28.40	0.98	3.61	53.98	5.41
100: 20	27.54	1.11	4.02	55.85	5.52
100: 22	26.38	1.23	4.41	56.71	5.72
100: 25	25.42	1.38	4.60	59.35	5.91

Based on laboratory experiments, it was shown that the introduction of ash ammonium nitrate into the melt makes it possible to obtain new nitrogen-potassium fertilizers with a high relative content of the assimilable form of K_2O.

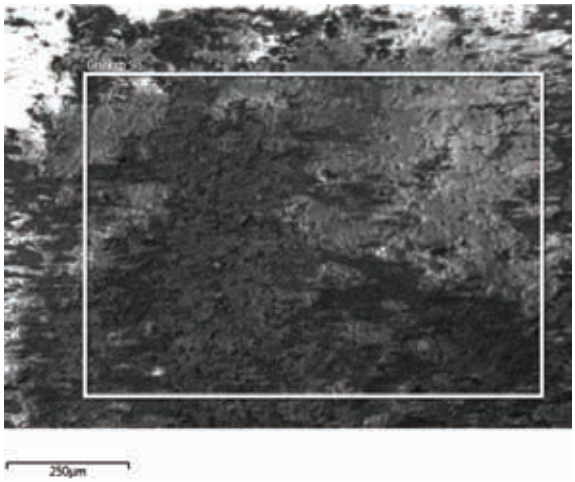

A

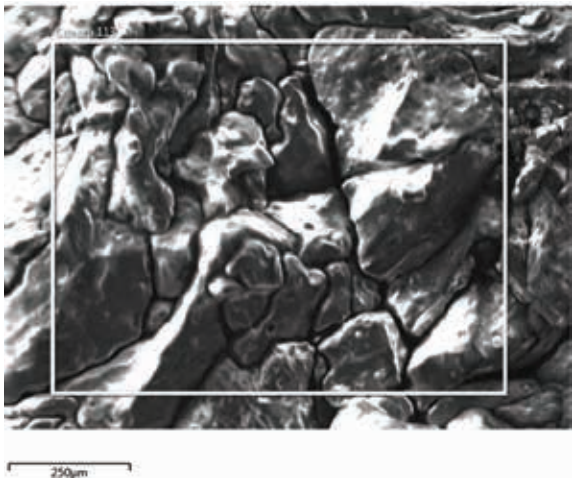

AC: K = 100: 3 ratio

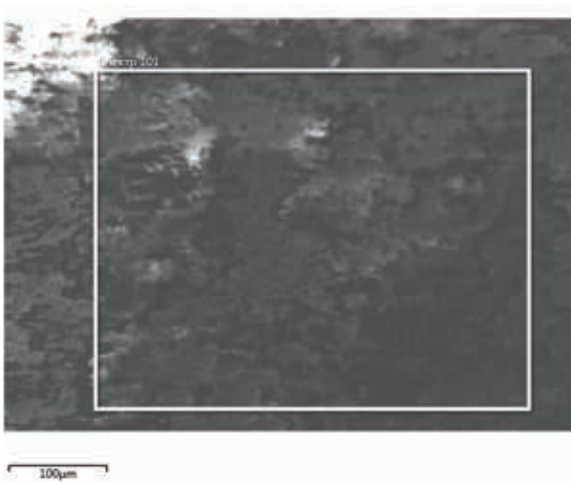

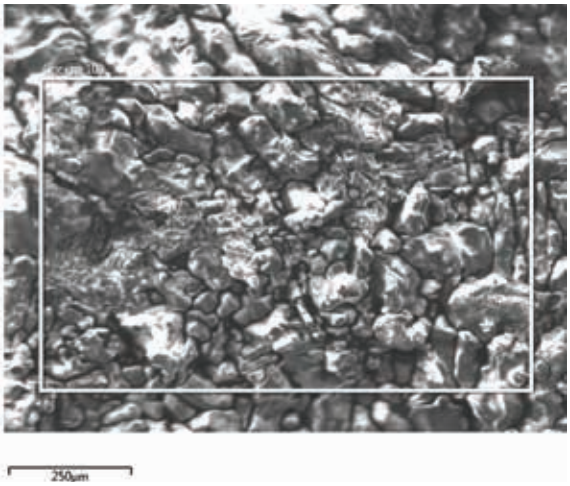

Б AC: K = 100: 3 ratio

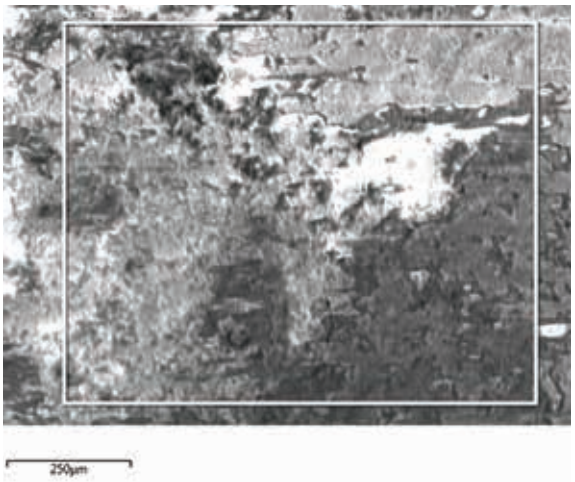

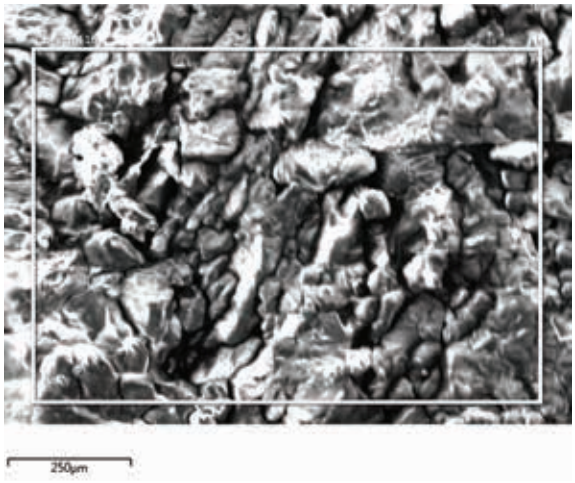

C AC: K = 100: 3 ratio

Figure 1. Electron microscopic photographs of the surface granules AC: sunflower (A); AU: Animal Dung (B) and AC: cotton stalk ash (C)

The rheological properties of saltpeter melts with sol were studied in the temperature range 160–185 °C. At the same time, it was shown that in all ratios of AS: Sol, potassium nitrate melts have a fairly good fluidity, which allows them to be granulated in a granulation tower by prilling without any special technological difficulties. Micrographs of granules of expanded ammonium nitrate of the obtained contact layer based on them. a) sunflower ash, (b) animal manure ash, (c) cotton stalk ash, on thermally expanded ammonium nitrate.

Conclusion

Thus, sunflower sol can be considered a very promising additive for the production of ammonium nitrate, which has a lower detonation stability.

References:

1. Marlair G. and Kordek M.-A. Safety and security issues relating to low capacity storage of AN-based fertilizers. Journal of Hazardous Materials,– 123(1–3). 2005.– P. 13–28.
2. Feick G. and Hainer R.M. On the thermal decomposition of ammonium nitrate. Steady-state reaction temperatures and reaction rate. Journal of the American Chemical Society,– 76(22). 1954.– P. 5860–5863.

3. Martorell S., Soares C. G. and Barnett J. Safety, Reliability and Risk Analysis: Theory, Methods, and Application // Volume 1. in European safety and reliability conference. ESREL 2008, and 17th SRA-EUROPE. September, 22–25, 2008. – Valencia, Spain: 2009. Taylor & Francis Group // URL: https://www.amazon.com/Safety-Reliability-Risk-Analysis-Applications/dp/ 0415485134.
4. Ammonium nitrate. Properties, production, application / A. K. Chernyshev, B. V. Levin, A. V. Tugolukov, A. A. Ogarkov, V. A. Ilyin. M. CJSC "INFOKHIM", 2009.– 544 p.
5. Glagolev O. L. Practical experience of operation of the AC-72 unit at OJSC "Cherepovets Azot" on a flexible scheme for the production of ammonium nitrate and products based on it // World of Sulfur, N, P and K.– No. 2. 2004.– P. 21–23.
6. Patent No. 2228322. Russia. Cl. From 05 G 1/06, From 05 to 11/06. Method for obtaining complex water-soluble fertilizers / L. V. Spakhova, L. P. Grosheva, N. V. Gorshkova, E. A. Maklashina, Yu. K. Samsonov, E. V. Lysenko, V.A. V. Balagurov, A. E. Pestov, S. P. Uvarov.– from 17.03.2003.
7. Patent No. 2253639 Russia. Cl. From 05 to 7/00, from 05 G 1/06, from 05 to 1/02. The method of obtaining granulated mineral fertilizer containing nitrogen and phosphorus, and granulated mineral fertilizer / V. A. Sezemin, O. B. Abramov.– B. I. 2005. – No. 16.
8. Guide to practical exercises on the technology of inorganic substances / M. E. Pozin., B. A. Kopylev., E. S. Tumarkina., G. V. Belchenko – L .: Goshimizdat, 1963.– 376 p.
9. Cherny V. A., Streltsov O. A. Application of aerosil for modification of nitrogen-containing mineral fertilizers // Chemical technology. 1988.– No. 2.– P. 47–49.
10. Uzakov O. A., Dehkanov Z. K., Aripov X. Sh. Obtaining Potassium Nitrate by the Conversion Method / Annals of the Romanian Society for Cell Biology. ISSN:1583–6258.– Vol. 25.– Issue 2. 2021.– P. 3164–3170. URL: http://annalsofrscb.ro/index.php/journal/article/view/1295
11. Erkinov R. B., Ismoilova G. I., Usmonova Z. Sh., Khusanov M. N. and Dekhkanov Z. K. Physical and chemical properties of ammonium nitrate with the addition of ash. Universum: technical sciences: scientific journal.– No. 4(85). 2021.– P. 68–70. URL: http://7universum.com/ru/tech/archive/category/485

https://doi.org/10.29013/AJT-22-7.8-36-41

Isakova Dilnoza T.,
Assistant, Department of Chemistry, Samarkand State Medical Institute
Aronbaev Sergey D.,
D. Sc., professor, Department of Chemistry, Samarkand State University
Aronbaev Dmitry M.,
Ph.D., Associate Professor, Department of Chemistry, Samarkand State University
Samarkand, University Boulevard

MODIFIED CARBON-CONTAINING ELECTRODES IN ELECTROANALYSIS: PAST, PRESENT AND FUTURE

Abstract. At the end of 2019, the scientific world celebrated the 60 th anniversary of the awarding of the Nobel Prize for his contribution to the development of electrochemistry to the Czech scientist Yaroslav Geyrovsky. The method of polarography developed by him opened a new page of quantitative and qualitative analysis in chemistry. This article is devoted to this event and provides brief information about the possibility of creating an alternative proposed by Geyrovsky to a dripping mercury electrode for polarographic analysis. In this context, the stages of development of electrochemical methods of analysis using carbon-containing materials will be presented here.

Keywords: Voltammetry, dripping mercury electrode, modified carbon-containing electrodes, stages of development of polarography.

Due to all its advantages: low cost, speed and simplicity, electrochemistry has always been an ideal choice for the quantitative analysis of substances of inorganic and organic nature. This was facilitated by the transition from the use of indicator dripping mercury electrodes in voltammetric analysis to solid carbon-containing ones [1].

Probably, the first idea of using carbon-graphite materials as electrodes for polarographic analysis was given by Adams, who proposed in 1959 to use a mixture of a paste-like consistency consisting of coal powder and a liquid non-electroactive binder. Since then, carbon paste electrodes (CPE) and the corresponding sensors have received attractive development in electrochemical analysis, in particular in voltammetry. The evolution of the development of voltammetry using paste and then modified electrodes is traced by the following stages [2].

- **1959–1963**: introduction of carbon paste and its first applications by Adams and his collaborators to study the mechanisms of electrode reactions of various organic compounds.
- **1964, 1965**: the first experiments on the modification of carbon pastes. The ability to vary the composition of carbon pastes and the relative ease of their preparation is a stimulating factor for changing the characteristics of the initial carbon-binder mixture by introducing other chemically active components into it, remains relevant today. It is this procedure that can lead to a purposeful improvement in the characteristics of the electrode.
- **1974:** the appearance of carbon pastes with an electrolytic binder. The replacement of conventional non-electroactive paste-like liquids with electrolyte solutions opened the

way for a certain branch of electrochemistry of electroactive electrodes made of carbon paste, which made it possible to study the redox behavior, as well as various structural and morphological changes of inorganic compounds dissolved directly in the electrolyte. Currently, such studies usually belong to a special field, the so-called solid-state electrochemistry.

- **1980–2000:** the era of chemically modified carbon pastes. Attempts to use favorable mechanical and electrochemical properties of carbon pastes for the manufacture of sensors of a new generation were crowned with success in the early 80s. Modification of carbon paste by impregnating carbon particles with a methanol solution of dimethylglyoxime represents another milestone in the history of CPE. This was the first attempt when a classical analytical reagent served as a selective modifier, thus initiating subsequent research on the development and application of chemically modified carbon paste electrodes (CMCPE) in electrochemical analysis [3].

Since then, the number of publications of works with chemically modified electrodes based on carbon-containing paste has begun to grow exponentially, including review articles. This trend continues at the present time.

In the late 80 s and early 90 s of the last century, works appeared on the modification of carbon-containing pastes with enzymes and other biologically active substances. On the basis of these pastes, enzymatic biosensors were created that allow controlling some enzymatically catalyzed reactions of biological substances. Initially, the enzyme immobilization procedure was carried out by simply adding the necessary enzyme to the carbon paste. The simplicity of making an enzyme sensor immediately attracted the attention of biochemists, and enzyme biosensors based on carbon paste quickly came to the fore. One of the first comprehensive reviews showing the entire genesis of such biosensors was presented by Gorton [4].

The 90 s and early 2000 s are characterized by the appearance of carbon-containing composites on the market, which allow replacing soft paste electrodes with hard ones. Usually, the method of manufacturing such solid electrodes differs little in simplicity from the manufacture of carbon paste electrodes, but the latter have a stronger matrix.

The 2000 s and up to the present – the period of development of methodological foundations for the modification of electrode materials; rejection of toxic mercury salts and other toxic components that pollute the environment and adversely affect human health; obtaining electrodes with a catalytic response that can significantly reduce overvoltage in the determination of a number of substances of inorganic, and especially organic nature; the use of noble metal nanoparticles and transition group metal oxides as modifying agents stimulated the development of a new direction in electrochemical analysis – nanoanalytics [5].

Carbon-containing nanomaterials based on mono- and poly-carbon nanotubes, nanopackages, graphitized nanofibers, etc., as well as nanorods made of precious metals have qualitatively new properties necessary for the creation of indicator electrodes: a large specific surface area, which determines their high electrochemical and catalytic activity, sorption properties, as a consequence of porosity and surface defects of nanomaterials, their thermal stability [6]. These properties of nanomaterials open wide horizons for further reducing the limits of determining trace amounts of matter in electroanalysis by using nanostructured electrodes, improving separation and concentration processes using nanotubes, nanostructured polymers as new selective sorbents. Currently, a series of electrochemical studies has been published in the analysis by voltammetry using various nanoparticles applied to the surface of the electrode as modifiers using physical sorption, chemisorption, laser ablation from solutions.

Such electrodes are able to exhibit an electrocatalytic effect in the redox processes of both organic and inorganic compounds by reducing the overvoltage of various electrode processes, increase the selectivity and sensitivity of electroanalysis. By sewing metal nanoparticles to DNA (an electrochemically inactive substance), pico- and nanomolar DNA concentrations can be determined [7]. Thick-film graphite electrodes modified by ex- or insitu bismuth film were used to determine trace amounts of zinc, cadmium and lead in multicomponent objects, group vitamins in pharmaceuticals [8; 9].

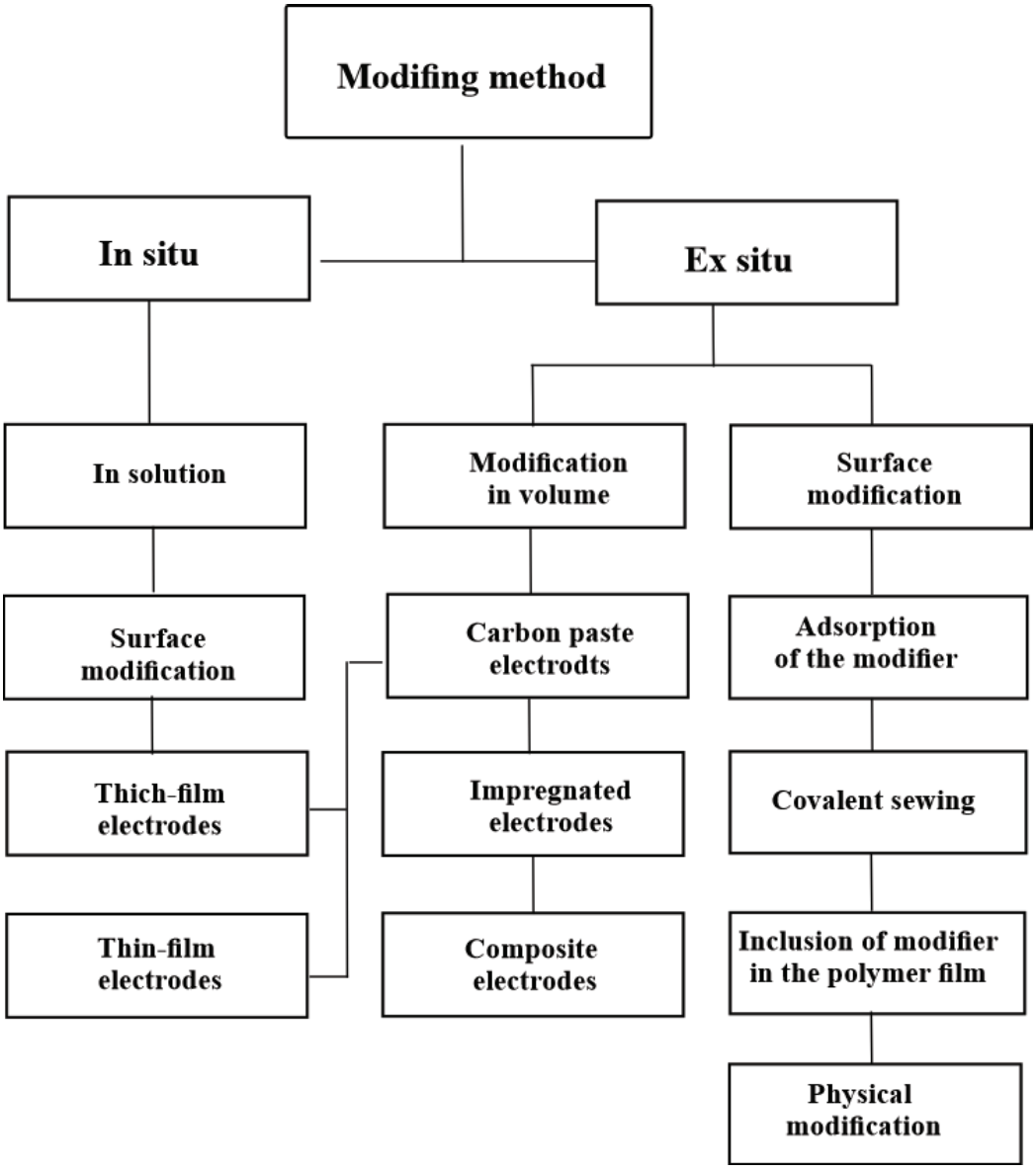

Fig.1. Methods of modification of electrodes

A thick-film carbon-containing electrode modified with silver nanoparticles was used for the inversion-voltammetric determination of sulfide ions and mercaptans in the contents of 10^{-7}–5×10^{-7} M, iodine in waters, food products and biological fluids in the concentration range of $1 \times 10^{-7} – 8 \times 10^{-7}$ M with a correlation coefficient of 0.9985. Gold and silver nanoparticles, silica gel with enzymes deposited on them, and nanotubes are used for electrochemical detection of biomolecules, including DNA in biosensors [10; 11].

Based on the specific electrochemical properties of metal nanoparticles, a new generation of highly sensitive sensors for environmental and medical purposes has recently been created. Thus, enzyme-free bio- and immunosensors based on Berlin azure nanolayers and magnetic nanoparticles have been tested [12].

The use of such biosensors opens up new possibilities for non-invasive methods of medical diagnostics [13; 14].

The main reason for the need to modify the electrode is to obtain a qualitatively new sensor with the desired, often predetermined properties. In this regard, carbon pastes can undoubtedly represent one of the most convenient materials for the manufacture of modified electrodes.

The methodology and principles of modification of carbon-containing pastes are illustrated by the scheme [7, 15] presented in (Fig. 1).

Unlike relatively complex modifications of solid substrates, the preparation of chemically modified carbon paste electrodes is very simple, usually using various alternative procedures. The modifier can be dissolved directly in the binder or mechanically mixed with the paste during its homogenization.

It is also possible to soak graphite particles with a modifier solution, and after evaporation of the solvent, use it as an impregnated carbon powder. Finally, already prepared pastes can be modified in situ.

The advantage of in situ modification methods is that they do not require the addition of modifier molecules to the electrode. It is enough to clean the surface from the products of the electrochemical reaction before modification. However, the service life of such electrodes is relatively short, since before each measurement there is a need for modification again.

As an alternative to in situ modification methods, methods of pre-immobilization of modifiers (ex situ) on electrodes made of various materials such as glass carbon, metals, pyrographite, carbon-containing composite materials, impregnated graphite, carbon mesh, carbon paste, fabrics, fibers, etc. have been developed and are widely used. The combination of their properties makes it possible to create electrodes with specified sensitivity and selectivity parameters.

Conclusion

Assessing the prospects of using modified electrodes in voltammetric analysis, it can be noted that the development of the method itself is increasingly mixed with the development of new electrodes and sensors that allow determining "cheaper, faster, easier and better". A large number of research works on the search for ways to use and select modifiers, their immobilization on the surface of electrodes, the use of electronic transfer mediators is an indisputable proof of interest in this problem, although the phenomenological stage in conducting research has not yet ended. A number of issues that prevent the widespread use of modified electrodes have not yet been resolved. In particular, this applies to the production of electrodes with a stable electrochemical response, which does not depend on the methods of preparing the electrode surface before the corresponding measurements. Attempts to replace mercury with other metals, for the most part, lead to a loss of sensitivity and selectivity of definitions.

The relatively short "life" of most electrodes, their "aging" over time, which manifests itself in changes in the composition and structure of the modifying layer and deterioration of its analytical characteristics, is another problem. The duration of operation of the electrodes is severely limited by the need to regenerate the surface after each measurement. It is the surface of the electrode that is the source of most problems. Even for a well-studied mercury film electrode (PRE), the nature of the mercury film on its surface is still being discussed – whether it is homogeneous with a thickness of 0.5 to 10 microns or Hg is released in the form of small droplets with a statistical distribution on the surface of the electrode.

When creating and using modified electrodes, it becomes necessary to answer a number of questions: how to make the surface of the modifying layer stable

and reproducible, how do the properties of the modifying layer affect the parameters of the response signal, how does electrochemical or mechanical surface treatment affect the activity of the modifier and the electrode process, how to eliminate contamination of the electrode with interfering substances, which worsens its analytical characteristics?

Thus, having considered various ways of modifying carbon-containing electrodes, we come to the following conclusions:

Chemical modification makes it possible to expand the analytical capabilities and scope of voltammetric analysis methods for the determination of various substances of inorganic and organic origin and to limit the use of mercury-containing electrodes. In the near future, the main task of electrochemical analysis methods is to improve the analytical parameters of electrodes with modification of their surface and the possibility of a catalytic response.

References:

1. Brainina H. Z., Neiman E. Ya., Slepushkin V. V. Inversion electroanalytical methods.– M.: Chemistry. 1988.– 56 з.
2. Svankara I., Vitras K., Kalcher K., Valkarius A., Van J. Carbon paste electrodes in facts, figures and notes: A retrospective review on the occasion of the 50th anniversary of carbon paste in electrochemistry and electroanalysis. Electroanalysis. – 21. 2009. – P. 7–28.
3. Kalcher K. Chemically modified carbon paste electrodes in voltammetric analysis // Electroanalysis. – 2. 1990. – P. 419–433. /doi.org/10.1002/elan. 1140020603
4. Gorton L. Electrodes made of carbon paste modified by enzymes, electroanalysis of tissues and cells. – Vol. 7. 1995. – P. 23–45. Doi.org/10.1002/elan. 1140070104
5. Zolotov Yu. A. Nanoanalytics // J. Anal.Chem.– Vol. 65.– No. 12.2010. – P. 1235–1236.
6. Aronbaev D. M., Aronbaev S. D., Narmaeva G. Z., Isakova D. T. Indicator carbon-paste electrode for voltammetric analysis // Industrial laboratory. Diagnostics of materials.–No. 2. 2020. – P. 5–14.
7. Budnikov G. K., Evtyugin G. A., Maistrenko V. N. Modified electrodes in voltammetry. chemistry, biology and medicine.– M.: Binom. Laboratory of knowledge. 2012.– 416 p.
8. Aronbayev S. D., Norkulov U. M., Narmayeva G. Z., Aronbayev D. M. Bismuth-modified electrodes in voltammetric analysis of organic compounds and biologically active substances: application experience and development prospects // Universum: Chemistry and Biology: electron. scientific. Journal. 2019. – No. 3(57).
9. Aronbayev S. D., Narmayeva G. Z., Aronbayev D. M. Investigation of the behavior of a carbon graphite electrode modified with a bismuth film in the voltammetric determination of vitamin B2 // Universum: Chemistry and biology: electron. scientific. journal. 2019. – № 3(57).
10. Wang J., Li J., Shi Z., Li N., Gu Z. Electrochemistry of DNA on single-walled carbon nanotubes // Electroanalysis.– Vol. 16.2004. – 140 p.
11. Pujado M. P. Carbon nanotubes as platforms for biosensors with electrochemical and electronic transduction © Springer-Verbs – Berlin Heidelberg, 2012.
12. Karyakin A. A. Highly effective biosensors for noninvasive diagnostics // Current biotechnology.– Vol. 26. – No. 3.2018. – P. 125–125.
13. Kozitsina A. N. Electrochemical sensor systems based on organic and inorganic nanoscale modifiers for enzyme-free determination of clinically significant compounds // Diss… doct.chemical sciences.- Yekaterinburg, 2018.– 343p.

14. Pribil M. M. Highly effective lactate biosensors based on immobilized lactate oxidase engineering // Diss … Candidate of Chemical Sciences.– M.:, MSU.2015.– 163 p.
15. Narmayeva G., Aronbayev S., Aronbayev D. Achievements and problems of modification of electrodes for voltammetry // International Scientific Journal – Grantaalaya.– 6(7).2018. – P. 368–381. URL: https://doi.org/10.5281/ zenodo.1345218

https://doi.org/10.29013/AJT-22-7.8-42-47

Naubeev Temirbek Khasetullaevich,
PhD {Chemistry}, docent,
Head of Department "Oil & Gas Technology",
Karakalpak State University

Uteniyazov Karimbay Kuanishbaevich,
PhD {Chemistry}, docent,
Department "Organic and inorganic chemistry",
Karakalpak State University

Ramazonov Nurmurod Sheralievich,
S. Yu. Yunusov Institute of the Chemistry of Plant Substances
Doctor of Sciences, (in chemistry), Professor,
Head of the laboratory Chemistry of glycosides
Academy of Sciences of Uzbekistan

TRITERPENE GLYCOSIDES *ASTRAGALUS* AND THEIR GENINS XCV. CYCLOASCIDOSIDE B FROM *ASTRAGALUS MUCIDUS*

Abstract. Structure of the novel cycloartane glycoside, cycloascidoside B isolated from the aerial parts of *Astragalus mucidus* Bunge (*Leguminosae*) is determined as 3-O-β-D-(2-OAc)-xylopyranoside, 6,25-di-*O*-β-*D*-glycopyranosides-24R-cycloartan-3β,6α,16β,24,25-pentanol. Structure of this glycoside had been proven based on chemical transformations and spectral data of NMR1H, ^{13}C.

Keywords: *Astragalus mucidus* Bunge, *Leguminosae*, cycloartan triterpenoids, cycloascidoside A, B and E, cycloasgenin C, spectra NMR^{1}H, ^{13}C, DEPT.

Continuing of our investigation of isoprenoid compounds from *Astragalus* (*Leguminosae*) plants and their chemical transformation [1], from the aerial part of *Astragalus mucidus* Bunge we have isolated a novel cycloarrtane glycoside named by us as cycloascidoside B (**1**). In the article we give proof of the chemical structure of the isolated glycoside.

NMR^{1}H spectrum of the novel glycoside **1** in high field at δ 0.07 and 0.45 have two single-proton doublets is discernible with specific germinal spin-spin coupling constant (SSCC) ^{2}J = 4 hz and signal of seven methyl groups at δ 0.83 – 1.86. These data indicate that the isolated compound is cycloartane type triterpene glycoside [2–5].

NMR^{1}H and ^{13}C spectrum have singlet signal of three proton units at 1.91 and signals of carbon atoms at 21.18 and 170.07. These data confirm that cycloascidoside B contains one acetyl group (table 2).

Acidic hydrolysis of glycoside **1** gives genine (**2**) identified with cycloasgenin C [1–8]. Sugar fraction of the yield of acidic hydrolysis contains *D*- glucose and *D*- xylose (lyxosazone) which are determined by paper chromatography method (PC) in the presence of samples of different carbohydrates.

Alkaline hydrolysis of cycloascidoside B (**1**) gives glycoside **3** identified with cycloascidoside E (**3**). Consequently, cycloascidoside B (**1**) is monoacetate of cycloascidoside E (figure 1) [8].

Partial hydrolysis of glycoside **3** gives cycloasgenin **2** and progenins **4** and **5**.

On basis of physical and chemical constants, spectral data and results of TLC analysis monoside

5 was identified as 3-*O*-β-*D*- xylopyranoside of cycloasgenin C [3], and bioside **4** was identified as cycloascidoside A (figure 1) [1].

NMR ^{1}H and ^{13}C spectra of cycloascidoside B (**1**) have signals of three protons at 4.67; 4.81; 5.08 and signals of three anomeric carbon atoms of monosaccharide residue at 104.96; 104.62 and 98.57.

Thereby, the above mentioned datum confirm that the cycloascidoside B (1) is trioside.

Comparative analysis of ^{13}C NMR spectrum data of cycloasgenin C (**2**) and cycloascidoside B (**1**) gives evidence that carbon atom C-3, C-6 and C-25 of cycloascidoside B (**1**) are endured glycosilation and resonate at 88.90; 79.14 and 80.86. These data shows that sugar residues are connected to genin through hydroxyl groups at C-3, C-6 and C-25 carbon atoms.

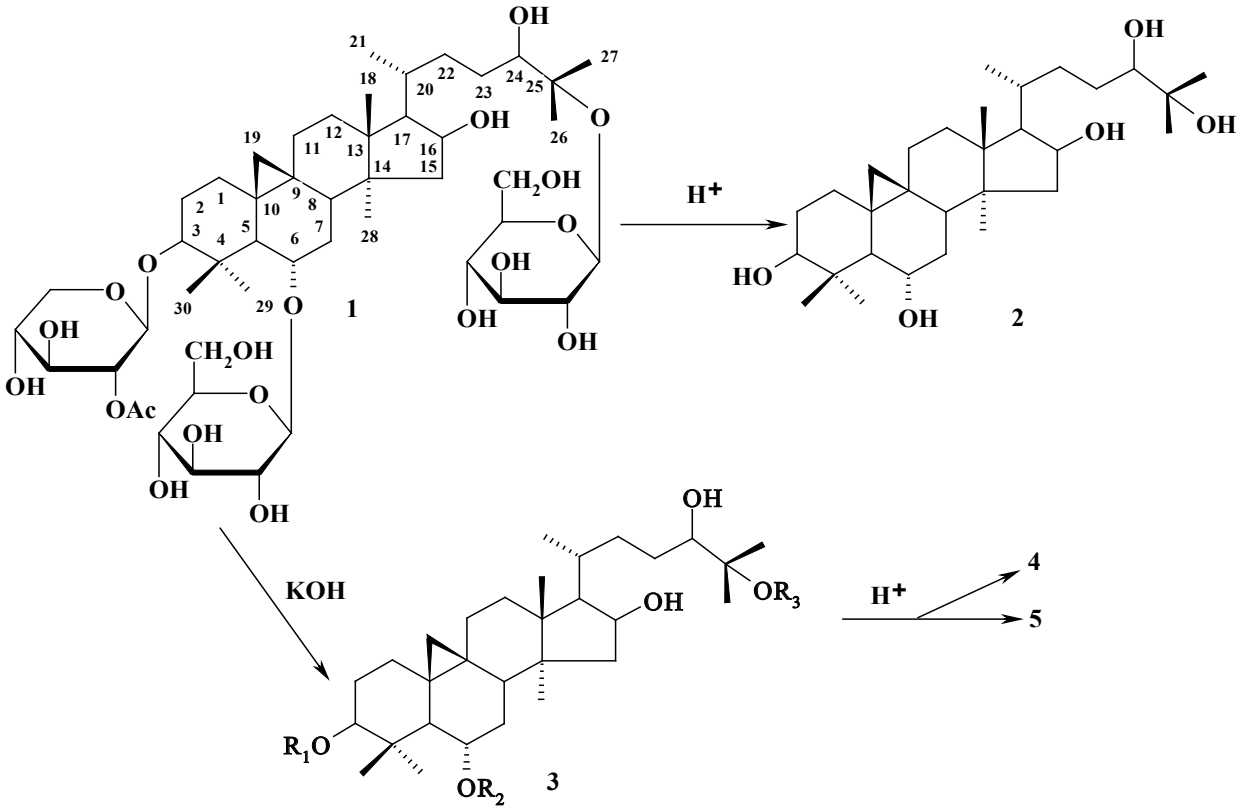

3. R_1=Xylp, R_2=R_3=Glcp
4. R_1=Xylp, R_2=Glcp, R_3=H
5. R_1=Xylp, R_2=R_3=H

Figure 1. Acidic and alkaline hydrolysis of cyclolastioside B (1)

Position of acetyl group in the molecule of isolated glycoside were found on basis of comparative analysis of ^{1}H and ^{13}C NMR spectra of compounds **1** and **3**. Comparative analysis of chemical shifts of anomeric carbon atoms in ^{13}C NMR spectra confirms position of acetyl group in the molecule of cycloascidoside B (**1**) at C-2^{1} atom of xylose (table 2). In ^{13}C NMR spectrum of cycloascidoside B (**1**) anomeric carbon atom C-1^{1} resonates at 104.96. Comparing of these data in cycloascidoside E (**3**) shows that atom C-1^{1} of xylose in cycloascidoside B (**1**) have endured diamagnetic displacement (shift) to 1.41. This data shows that acetyl residue is located in molecule of xylose. Value of upfield shift of carbon atom C-1^{1} indicates that acetyl group attached to carbon atom C-2^{1}. This conclusion is also proved out by

upfield shift of signal C-3[1] to 2,93. Abovementioned data let us to make conclusion that acetyl group in cycloascidoside B (**1**) is attached at C-2[1] of xylose.

Analysis of ^{1}H and ^{13}C NMR spectra (table 2) of glycoside **1** shows, that it has three monosaccharide residue and is trioside.

Table 1.– ^{13}C NMR data of aglycone part of cycloascidoside B (1), cycloasgenin C (2), cycloascidoside E (3), cycloascidoside A (4) and 3-*O*-β-*D*- xylopyranoside of cycloasgenin C (5) (C_5D_5N, δ, J/Hz)

Atom C	DEPT	1	2 [3]	3	4	5 [3]
1	CH_2	32.01	32.83	32.20	32.20	32.97
2	CH_2	29.83	31.45	30.22	30.18	30.85
3	CH	88.90	78.41	88.55	88.55	89.20
4	C	42.18	42.45	42.65	42.64	43.20
5	CH	52.37	54.05	52.48	52.49	54.61
6	CH	79.14	68.35	79.16	79.16	68.40
7	CH_2	34.35	38.62	34.23	34.24	38.93
8	CH	45.64	47.27	45.62	45.59	47.50
9	C	21.40	21.34	21.38	21.41	21.84
10	C	28.63	29.67	28.71	28.73	29.71
11	CH_2	26.17	26.43	26.26	26.29	26.79
12	CH_2	33.08	33.28	33.14	33.14	33.64
13	C	45.74	45.78	45.66	45.75	46.19
14	C	46.80	47.00	46.89	46.99	47.41
15	CH_2	48.00	48.83	48.05	48.19	49.20
16	CH	71.70	71.83	71.75	71.69	72.20
17	CH	57.17	57.31	57.15	57.02	57.70
18	CH_3	18.51	18.80	18.47	18.50	19.27
19	CH_2	30.02	30.40	30.33	28.16	30.46
20	CH	31.46	31.66	31.55	31.63	32.11
21	CH_3	18.72	19.10	18.80	18.82	19.46
22	CH_2	34.86	34.86	34.96	34.82	35.31
23	CH_2	29.18	29.43	29.25	29.32	29.86
24	CH	78.88	80.58	78.94	80.58	81.07
25	C	80.86	72.71	80.56	72.67	73.16
26	CH_3	21.58	25.86	21.50	25.95	26.41
27	CH_3	24.13	26.22	24.22	26.10	26.64
28	CH_3	19.80	20.31	19.83	19.86	20.70
29	CH_3	28.44	29.34	28.52	28.53	29.36
30	CH_3	16.49	16.12	16.63	16.64	17.18

Anomeric protons of monosaccharide residue are resonated in ^{1}H NMR spectra of glycoside 1 at δ 4.67 (H-1 of residue of β-*D*-xylopyranoses, d, ^{3}J = 8 Hz), δ 4.81 (H-1 of residue of β-*D*- glucopyranose, d, ^{3}J =7.5 Hz) and δ 5.08 (H-1 of residue of β-*D*-glucopyranose, d, ^{3}J=7.6 Hz) (table 2). It means that monosaccharide residues in the glycoside have pyranose form, $^{4}C_1$- conformation and β-configuration of chemical structure. This conclusion is also confirmed by chemical shift value of carbon atoms of monosaccharide residues in ^{13}C NMR spectra of cycloascidoside B. Mentioned values of ^{13}C NMR also point at terminal character of both monosaccharide residues. Accordingly, cycloascidoside B is trisdesmoside glycoside.

Table 2. – ^{13}C NMR data of carbohydrate part of cycloascidoside B (1), cycloascidoside E (3), cycloascidoside A (4) and 3-*O*-β-*D*- xylopyranoside of cycloasgenin C (5) (C_5D_5N, δ, J/Hz)

Atom C	**3-O-β-D-Xylp**			
1	104.96	106.37	107.63	108.12
2	76.13	75.57	75.59	76.13
3	75.52	78.45	78.51	79.02
4	71.23	71.22	71.23	71.74
5	66.98	66.99	67.03	67.55
Ac	21.18			
	170.07			
6-O-β-D-Glc*p*				
1	104.62	105.54	105.18	
2	75.52	75.57	75.59	
3	79.00	79.13	79.16	
4	71.70	71.77	71.83	
5	77.95	78.14	78.09	
6	63.02	63.07	63.12	
25-O-β-D-Glc*p*				
1	98.57	98.45		
2	75.23	75.40		
3	78.57	78.54		
4	71.79	71.77		
5	78.05	78.24		
6	62.69	62.66		

According to comparative analysis of ^{13}C NMR spectra of compounds 1 and 2 location of residue of D-xylopyranose found be at C-3, and location of D-glucopyranose residues at C-6 and C-25. From table 1, signal of carbon atom C-3 have downfield shift to 10.49, and signals of C-6 and C-25 carbon atoms have downfield shift to 10.79 and 8.15 comparatively with cycloasgenin C.

Anomeric carbon atoms of monosaccharide residues resonate at δ104.96 (C-1 of β-*D*-xylopyranoses), 104.62 (C-1 of β-D-glucopyranose) and 98.57 (C-1 of β-*D*-glucopyranose) in ^{13}C NMR spectra of cycloascidoside E. Chemical shift values of anomeric carbon atoms show that residue of *D*-xylose is attached to C-3, and residues of *D*-glucose are attached to C-6 and C-25 of genin.

Thereby, on basis of above described experimental data the chemical structure of isolated novel cycloartane line triterpene glycoside, cycloascidoside B is 3-*O*-β-*D*-(2-OAc)- xylopyranoside, 6,25- di-*O*-β-*D*-glycopyranosides-24R-cycloartan-3β, 6α,16β, 24, 25-pentaol.

Experimental part. General Experimental Procedures [1]. Following solvent systems were used: chloroform – methanol – water, 70:12:1 (1), chloroform – methanol, 9 : 1 (2), chloroform – methanol – water, 70 : 23 : 3 (3). NMR spectrum of the compounds were recorded on Unityplus 400 (Varian) referenced with respect to the residual solvent signal of C_5D_5N. ^{13}C NMR spectrum were recorded at complete suppression of C-H interaction and under DEPT conditions. Chemical shifts of protons of compositions **1**, **3** were described in reference to HMDS.

Extraction and isolation. Isolation method of isoprenoids from aerial part *Astragalus mucidus* Bunge were given in [1]. 150 mg (0.01%) of cycloascidoside B was isolated by elution of silica gel column with the system 3.

Cycloascidoside B (1), $C_{49}H_{82}O_{21}$, melting point. 280–282°C (from methanol). Spectra NMR1H (400 MHz, C_5D_5N, δ, ppm., J/hz): 0.07, 0.45 (each 1H, d, J=4, H-19), 0.83 (3H, c, Me-28), 0.95 (3H, d, J=6.4, Me-21), 1.24, 1.25, 1.37, 1.38, 1.86 (each 3H, c, Me-30, 18, 27, 26, 29), 1.91 (3H, s, OAc), 3.41 (1H, dd, J=11.6, 4.9, H-3), 3.57 (1H, dd, J=11.3, 10, H-5α, Xyl*p*), 3.68 (1H, td, J=9, 3.8, H-6), 3.78 (1H, ddd, J=9.2, 5.1, 2.7, H-5 Glc*p*), 3.84 (1H, m, H'-5, Glc*p*,), 3.86 (1H, dd, J=8.4, 7.8, H'--2, Glc*p*), 3.93 (1H, dd, J=8.9, 7.8, H-2, Glc*p*), 4.00 (1H, t, J=8.5, H-3, Xyl*p*), 4.04 (1H, t, J=8.8, H-3', Glc*p*), 4.06 (1H, t, J=8.9, H-4, Glc*p*), 4.08 (1H, t, J=8.9, H-4, Xyl*p*), 4.09 (1H, t, J=8.7, H'-4, Glc*p*), 4.11 (1H, t, J=8.9, H-3, Glc*p*), 4.20 (1H, dd, J=11.7, 5.5, H-6, Glc*p*), 4.20 (1H, dd, J=11, 5.1, H-5e, Xyl*p*), 4.38 (1H, dd, J=11.7, 3.1, H-6, Glc*p*), 4.40 (1H, dd, J=11.6, 2.6, H-6', Glc*p*), 4.52 (1H, td, J=7.6, 5.2, H-16), 3.76 (1H, dd, J=10.5, 2, H-24), 4.67 (1H, d, J=8, H-1, Xyl*p*), 4.81 (1H, d, J=7.5, H-1, Glc*p*), 5.08 (1H, d, J=7.5, Glc*p*, H-1), 5.40 (1H, dd, J=8.8, 8, Xyl*p*, H-2). For Spectra ^{13}C refer to table 1, 2.

Acidic hydrolysis of cycloascidoside B. Glycoside **1** (30 mg) was dissolved in 10 ml of methanol that contains 0.5% of sulfuric acid, and boiled it in boiling-water bath for 1 hour. Then the reaction mixture was diluted with water up to 30 ml and MeOH was evaporated. Formed sediment was filtered, washed with water and dried. Filtrate was neutralized with $BaCO_3$. After removing of precipitate the solvent was concentrated and analyzed by TLC method using solvent system 3 and in comparison with samples *D*-glucose and *D*- xylose were found.

Residue was rechromatographed silica gel column by eluating with system 2. Genin **2** (15 mg) identified with cycloasgenin C in comparison with samples by TLC analysis and on basis of ^1H NMR spectrum.

Cycloasgenin C. ^1H NMR spectra (400 MHz, C_5D_5N, δ, ppm, J/hz): 0.21, 0.49 (each 1H, d, J=4, H-19), 0.92 (3H, s, Me-28), 1.00 (3H, d, J=6.4, Me-21), 1.25, 1.30, 1.36, 1.39, 1.77 (3H, c, Me-30, Me-18, Me-27, Me-26, Me-29), 3.55 (1H, dd, J=11.4, 4.7, H-3), 3.67 (1H, dd, J=10.4, 2.3, H-24), 3.69 (1H, td, J=9.4, 3.7, H-6), 4.60 (1H, td, J=7.8, 5.0, H-16).

Alkaline hydrolysis of cycloascidoside B. Cycloascidoside B (**1**) 50 mg was saponified in 20 ml of 0,5% methanol solution of potassium hydroxide. Reaction mixture was set at room temperature during 24 hour, then diluted with 25 ml of water. Then the mixture was neutralized with acetic acid. MeOH was evaporated and extracted with BuOH. The obtained residue was rechromatographed with silica gel. 30 mg of cycloascidoside E (**3**) was isolated by eluating with system 3, $C_{47}H_{80}O_{19}$, mp 276–278 °C (from MeOH). ^1H NMR spectra of cycloascidoside E (400 MHz, C_5D_5N, δ, ppm, J/Hz): 0.06, 0.45 (each 1H, d, J=4, H-19), 0.84 (3H, s, Me-28), 0.96 (3H, d, J=6.4, Me-21,), 1.23, 1.25, 1.38, 1.39, 1.91 (3H, s, Me-30, Me-18, Me-27, Me-26, Me-29), 3.40 (1H, dd, J=11.6, 4.3, H-3,), 3.56 (1H, dd, J=11.3, 10, H--5α Xyl*p*), 3.67 (1H, td, J=8.4, 4.3, H-6,), 3.77 (1H, dd, J=10.5, 2, H-24,), 3.78 (1H, ddd, J=9.2, 5.1, 2.7, Glc*p* H-5), 3.85 (1H, m, Glc*p* H'-5), 3.87 (1H, dd, J_1=8.4, 7.9, Glc*p* H'-2), 3.92 (1H, dd, J=8.6, 7.5, Glc*p* H--2), 3.93 (1H, dd, J=8.6, 7.5, Xyl*p* H-2), 4.03 (1H, t, J=8.6, Xyl*p* H-3), 4.05 (1H, т, J=8.9, Glc*p* H-4), 4.06 (1H, t, J=8.8, Glc*p* H'-3), 4.09 (1H, t, J=8.9, Xyl*p* H-4), 4.10 (1H, t, J=8.7, Glc*p* H'-4), 4.11 (1H, t, J=8.9, Glc*p* H-3), 4.20 (1H, dd, J=11.7, 5.5, Glc*p* H--6), 4.21 (1H, dd, J=11.5, 5.1, Xyl*p* H-5e), 4.35 (1H, dd, J=11.6, 3, Glc*p* H-6), 4.38 (1H, dd, J=11.6, 2.6, Glc*p* H'-6), 4.54 (1H, td, J=7.7, 5.3, H-16), 4.76 (1H, d, J=7.8, Glc*p* H-1). 4.79 (1H, d, J=7.5, Xyl*p* H-1), 5.06 (1H, d, J=7.8, Glc*p* H'-1). ^{13}C NMR spectrum of cycloascidoside E is given in tables 1, 2.

Partial hydrolysis of cycloascidoside E. Glycoside **3** (30 mg) was dissolved in 100 ml of methanol that contains 0.5% of sulfuric acid, and boiled it in boiling-water bath for 1 hour. The reaction mixture was diluted with water up to 30 ml and MeOH was removed by evaporation. Formed precipitation was filtered, washed with water and dried. Filtrate was

neutralized with $BaCO_3$. Filtrate was analyzed by TLC method using system 3 in comparison with samples and found *D*-glucose and *D*-xylose.

Residue was set to column with silica gel and was eluated with system 2. Genin **2** (7 mg) was isolated and identified with cycloasgenin C by TLC method and according to information of ^{1}H NMR spectrum.

Monoside **5** (8 mg) (3-*O*-β-*D*- xylopyranoside of cycloasgenin C), $C_{35}H_{60}O_9$, mp 252–254°C (from MeOH) and bioside **4** were isolated by eluting the silica gel column with system 1 [1; 3]. ^{1}H NMR spectra of progenin **5** (400 MHz, C_5D_5N, δ, ppm, J/Hz): : 0.30, 0.58 (each 1H, d, J=4, H-19), 1.05 (3H, s, Me-28), 1.13 (3H, d, J=6.4, Me-21), 1.36, 1.42, 1.51, 1.53, 2.02 (3H, s, Me-30, Me-18, Me-27, Me-26, Me-29), 3.60 (1H, dd, J=11.2, 9.8, Xyl*p* H-5*a*), 3.64 (1H, dd, J=11.7, 4.6, H-3), 3.67 (1H, td, J=9.7, 3.6 H--6), 3.75 (1H, dd, J=10.5, 2.4, H-24), 3.83 (1H, dd, J=8.8,7.5,Xyl*p*H-2),4.06(1H,t,J=8.6,Xyl*p*H-3),4.15 (1H, m, Xyl*p* H-4), 4.36 (1H, dd, J=11.3, 5, Xyl*p* H--5*e*), 4.71 (1H, td, J=7.7, 4.9, H-16), 4.92 (1H, d, J=7.5, Xyl*p* H-1). For spectra ^{13}C NMR spectra of progenin 5 is given in the (table 1).

Progenin 4. ^{1}H NMR spectra (400 MHz, C_5D_5N, δ, ppm, J/Hz): 0.06, 0.45 (each 1H, d, J=4.3, H-19), 0.85 (3H, s, Me-28), 0.97 (3H, s, J=6.4, Me-21,), 1.24, 1.26, 1.36, 1.39, 1.90 (3H, s, Me-30, Me-18, Me-27, Me-26, Me-29), 3.40 (1H, dd, J_1=11.6, 4.3, H-3), 3.56 (1H, dd, J=11.3, 10, Xyl*p* H-5*a*), 3.67 (1H, dd, J=10.5, 2.4, H-24), 3.68 (1H, td, J=8.4, 4.3, H-6), 4.57 (1H, td, J=7.5, 4.9, H-16), 3.77 (1H, ddd, J=9.2, 5.1, 2.7, Glc*p* H-5), 3.91 (1H, dd, J=8.9, 7.8, Glc*p* H-2), 3.92 (1H, dd, J=8.6, 7.5, Xyl*p* H-2), 4.02 (1H, t, J=8.6, Xyl*p* H-3), 4.09 (1H, m, Xyl*p* H--4), 4.11 (1H, t, J=8.9, Glc*p* H-3), 4.19 (1H, dd, J=11.6, 5.4, Glc*p* H-6), 4.22 (1H, dd, J=11.5, 5.1, Xyl*p* H-5*e*), 4.35 (1H, dd, J=11.6, 3, Glc*p* H-6'), 4.71 (1H, d, J=7.5, Xyl*p* H-1), 4.79 (1H, d, J=7.8, Glc*p* H--1). ^{13}C NMR spectra of the progenin **4** is given in the (table 1).

References:

1. Naubeev T. Kh., Uteniyazov K. K., Isaev M. I. Chem. Nat. Compd.,– 47. 2011.– 250 p.
2. Naubeev T. Kh., Zhanibekov A. A., Isaev M. I. Chem. Nat. Compd.,– 48. 2012.– 813 p.
3. Naubeev T. Kh., Zhanibekov A. A., Uteniyazov K. K., Bobakulov Kh.M., Abdullaev N. D. Chem. Nat. Compd.,– 49. 2014.– 1048 p.
4. Naubeev T. Kh., Uteniyazov K. K., Tlegenov R. R., Uteniyazov K. J. Uzbek Chemical Register,– 29. 2008.
5. Isaev M. I., Gorovits M. B., Abdullaev N. D., Abubakirov N. K. Chem. Nat. Compd.– 18, 1982.– 424 p.
6. Isaev M. I. Chem. Nat. Compd.,– 31. 1995.– 690 p.
7. Kucherbayev K. D., Uteniyazov K. K., Kachala V. V., Saatov Z., Shashkov A. S. Chem. Nat. Compd.– 38. 2002.– 447 p.
8. Naubeev T. X., Janibekov A. A., Kucherbayev K. Dzh. Uzb. Biol. J.,– 35. 2017.

https://doi.org/10.29013/AJT-22-7.8-48-53

Radjabov O. I.,
Institute of Bioorganic Chemistry AS RUz, Tashkent, Uzbekistan
Turaev A. S.,
Institute of Bioorganic Chemistry AS RUz, Tashkent, Uzbekistan
Otajanov A. Yu.,
Institute of Bioorganic Chemistry AS RUz, Tashkent, Uzbekistan
Muydinov N. T.,
Andijan State State Pedagogical Institute, Andijan, Uzbekistan
Avezov H. T.,
Bukhara State University, Bukhara, Uzbekistan
Ruzieva M. J.,
Bukhara State University, Bukhara, Uzbekistan
Azimova L. B.,
Institute of Bioorganic Chemistry AS RUz, Tashkent, Uzbekistan
Buriev D. A.,
Institute of Bioorganic Chemistry AS RUz, Tashkent, Uzbekistan

STUDY OF PHYSICO-CHEMICAL PROPERTIES OF BIOMATERIAL OBTAINED BASED ON STRUCTURED COLLAGEN

Abstract. The article presents the results of the study of the physicochemical properties of the biomaterial in the form of a film based on collagen, obtained from the hide of cattle with the preservation of the original fibrous structure, and Na-CMC. The temperature dependence of the rheological properties of collagen, as well as compositions based on collagen and Na-CMC in different mass ratios, was studied. To study the preservation of the three-helix structure of collagen, the dynamic viscosity of aqueous solutions of collagen and compositions based on it were studied at temperatures of 30 and 35°C. It has been established that at a temperature of 35 °C the native structure of collagen is destroyed. The optimum temperature for the formation of a biomaterial based on an aqueous composition of collagen/polysaccharide in the form of a film is less than 30 °C. It is shown that the presence of a plasticizer significantly affects the mechanical properties of the films. When glycerol was added as a plasticizer to aqueous solutions of the collagen/Na-CMC composition, the formation of a highly elastic film was observed. When studying the dissolution time of the experimental samples, it was shown that with an increase in the mass fraction of Na-CMC in the composition of the film, a decrease in swelling and an increase in the dissolution time are observed due to the formation of intermolecular hydrogen bonds between the functional groups of collagen molecules and Na-CMC.

Keywords: collagen; polysaccharide; composition; viscosity; film.

1. Introduction

Collagen contains a significant number of diverse functional groups that can interact with medicinal substances and form complexes, the stability of which is determined by many factors. In addition, collagen macromolecules with an asymmetric three-helical conformation are prone to aggregation with the formation of supramolecular fibrous structures built from fibrillar elements, which can also cause the inclusion of various drugs in their composition [1].

Collagen has long been used in wound care as a wound dressing in various forms such as powder, amorphous gels/pastes, gel-impregnated dressings, and pads. In the skin, collagen peptides act as false collagen degradation peptides that send a false signal to fibroblast cells to synthesize new collagen fibers. In addition, collagen peptides have chemotactic properties; they can promote cell migration and proliferation, which is an important process in wound healing [2–4]. Abroad in 1959, for the first time, films reconstructed from a collagen solution were used for the treatment of wounds [5]. Subsequently, several researchers in the experiment and clinic showed the effectiveness of the use of film materials from bovine skin collagen in the treatment of wounds of the skin and internal organs [6–7]. Employees of the 1st Moscow Medical Institute. THEM. Sechenov and the Institute of Light Industry 1963 began research on the study of plastic materials based on type I collagen obtained from the dermis of cattle [8–10].

Biocompatibility and biodegradability are two important parameters to consider when choosing a polymer for its biomedical use. Biocompatibility refers to the specific properties of a material that does not have toxic or harmful effects on biological systems. Biocompatible polymers for pharmaceutical dosage forms have allowed the advancement of pharmaceuticals, providing better therapy [11–13].

When developing new medical biomaterials and improving formulations and technology, pharmaceutical factors are of particular importance. One of them is the biomaterial shapers, which can provide the structural and mechanical properties of the dosage form, create an optimal microenvironment for wound regeneration, have an absorption capacity for excess wound exudate, contribute to the creation of optimal wound surface moisture, and have sufficient mechanical performance [14].

To obtain a medical biomaterial in the form of a film based on collagen, it is necessary to choose a biocompatible polysaccharide with collagen. Since due to the high viscosity of the water mass of collagen, it is impossible to obtain a biomaterial in the form of a film, we have conducted studies on the preparation of an aqueous composition of collagen and Na-CMC.

The purpose of this work is to study the physicochemical properties of a biomaterial obtained based on structured collagen.

2. Materials and Methods

2.1. Material

The object of the study was the aqueous mass of neutral collagen isolated from the skin of cattle (dry residue 4.5–5%) [15] and sodium salt of carboxymethylcellulose (Na-CMC) with a degree of polymerization of 530 and a degree of substitution for $-CH_2COONa$ groups of 85%.

2.2. Obtain a composition

Distilled water was added to the neutral aqueous mass of collagen (dry residue 4.5–5%), up to a collagen concentration of 1.5%, and Na-CMC powder was added by stirring in different mass ratios. Mixing was carried out at room temperature for 30 min until the components were completely dissolved and a homogeneous dough-like mass was formed.

2.3. Obtain the film

Glycerol was added to the aqueous composition as a plasticizer and mixed on a magnetic stirrer at room temperature for 10 min, the mixture was poured into a mold and dried at room temperature not exceeding 30 °C.

2.4. Studies of the rheological properties

Studies of the rheological properties of aqueous solutions of collagen and the composition were

carried out on a rotational viscometer HAAKE Viscotester 2 plus, at temperatures of 20, 25, 30, and 35 °C.

2.5. Determination elasticity of film

The elasticity of the film was determined visually by the absence of adhesion or brittle fracture when the film was folded 180° ("++" – elastic; "+" – elastic, but elastic when folded; "–" – no elasticity).

2.6. Determination of geometric dimensions

The geometric dimensions of the film were measured with a micrometer with a division value of 0.01 mm according to OST 64–072–89.

2.7. Film dissolution time determination

The dissolution time of the film was evaluated by dissolving with continuous stirring film samples of 2 × 2 cm in 20 ml of purified water (temperature 37 ± ± 2 °C) and measured the time of complete dissolution in minutes.

2.8. Determination of the pH of the aqueous extract

The pH of the aqueous extract of the film was determined potentiometrically at a temperature of 20 °C.

3. Results

It is known from the literature data that an increase in temperature to 30 °C leads to a conformational change in the structure of collagen helices, accompanied by a "helix-coil" transition, as a result of which the supramolecular structure of collagen solutions also changes, and the viscosity and structural parameters drop sharply [16]. When aqueous solutions of collagen are heated to 30 °C and higher, a sharp irreversible decrease in viscosity is observed, a change in the structure of the collagen molecule, and denaturation also occurs. Therefore, during our research, the temperature dependence of the rheological properties of collagen, as well as compositions based on collagen and Na-CMC in different mass ratios, were studied (Figures 1, 2).

4. Discussion

As can be seen from figure 1, at temperatures of 20 and 25 °C, there are no sharp changes in the dynamic viscosity of collagen and compositions based on collagen/Na-CMC.

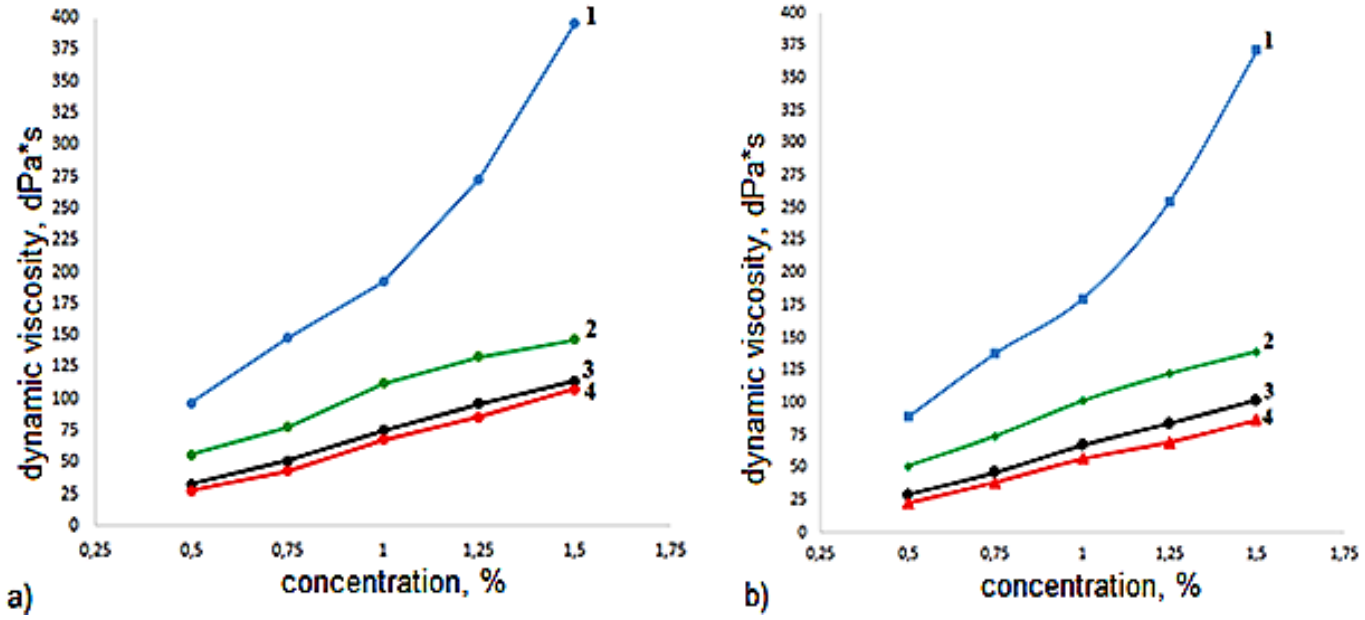

Figure 1. Dynamic viscosity at temperatures, a) 20°C; b) 25°C: 1 – collagen, 2 – collagen/Na-CMC80/20, 3 – collagen/Na-CMC75/25, 4 – collagen/Na-CMC70/30

To study the preservation of the three-helix structure of collagen, we studied the dynamic viscosity of aqueous solutions of collagen and compositions based on it at temperatures of 30 and 35 °C (Figure 2).

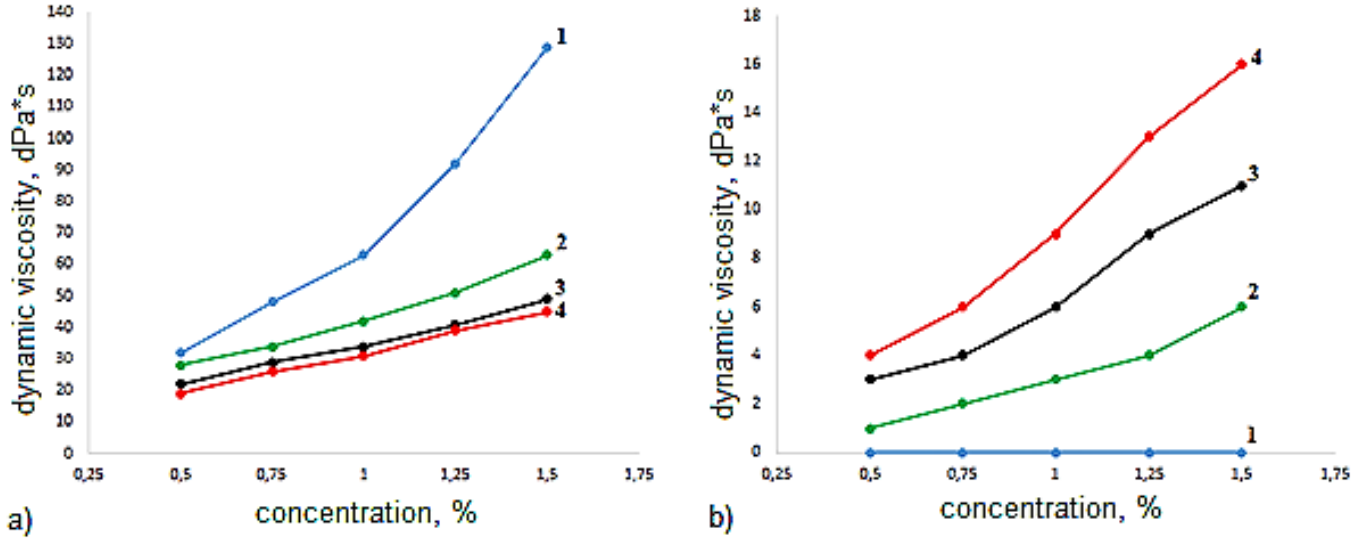

Figure 2. Dynamic viscosity at temperatures, a) 30ºC; b) 35ºC: 1 – collagen, 2 – collagen/Na-CMC80/20, 3 – collagen/Na-CMC75/25, 4 – collagen/Na-CMC70/30

As can be seen from figure 2, at temperatures of 30 and 35 °C there is a sharp change in the dynamic viscosity of collagen and compositions based on collagen/Na-CMC. However, at a temperature of 35 °C, the dynamic viscosity of an aqueous solution of collagen in all studied concentrations is equal to zero. These data indicate that at a temperature of 35 °C, the native structure of collagen is destroyed. The data obtained indicate that for the formation of biomaterial-based on collagen/polysaccharide in the form of a film, the optimum temperature is less than 30 °C.

To obtain a biomaterial based on collagen in the form of a film, glycerol was added to a homogeneous aqueous solution of the collagen/Na-CMC composition with stirring and poured into a mold at room temperature. The presence of a plasticizer significantly affects the mechanical properties of the films. It turned out that when glycerol is added as a plasticizer to aqueous solutions of the collagen/Na-CMC composition, the elasticity of the film increases. Glycerin conformed to the compositions and showed good plasticizing properties, which led to the formation of a highly elastic film.

Elasticity is one of the indicators of physiology, the ability of the coating to take the shape of the human body and come into contact with the entire surface of the tissues. All obtained film samples have good elasticity. The physical and mechanical properties of the studied films are shown in (Table 1).

Table 1.– Physical and mechanical properties of biopolymer films

№	Film composition	Elasticity	Thickness, mm	Density, g/cm^3	Dissolution time, min	the pH of water extract
1	Collagen-Na-CMC80/20	+ +	0,11	1,09	180	6.8
2	Collagen-Na-CMC75/25	+ +	0,11	1,07	over 200	6.9
3	Collagen-Na-CMC70/30	+ +	0,11	1,04	over 200	6.9

The study of the dissolution time of experimental film samples showed that with an increase in the mass fraction of Na-CMC in the composition of the film, a decrease in swelling and an increase in the dissolution time are observed, respectively. This is explained by the fact that intermolecular hydrogen bonds are formed between the functional groups of the collagen molecule and Na-CMC, and films based on them become stronger.

5. Conclusions

The temperature dependence of the rheological properties of collagen, as well as compositions based on collagen and Na-CMC in different mass ratios, was studied. It has been established that at a temperature of 35 °C the native structure of collagen is destroyed. The optimum temperature for forming a biomaterial based on collagen/polysaccharide in the form of a film is less than 30 °C. It is shown that the presence of a plasticizer significantly affects the mechanical properties of the films. When glycerol was added as a plasticizer to aqueous solutions of the collagen/Na-CMC composition, the formation of a highly elastic film was observed. It has been established that with an increase in the mass fraction of Na-CMC in the film composition, a decrease in swelling and an increase in the dissolution time are observed due to the formation of intermolecular hydrogen bonds between the functional groups of collagen molecules and Na-CMC.

References:

1. Istranov L. P., Istranova L. V., Sychenikov I. A. Structure, properties, uses of collagen in medicine. Pharmacy.– 5. 1984.– P. 76–79.
2. Hochstein A. O., Bhatia A. Collagen: its role in wound healing. Podiatry Manag. 2014.– P. 103–109.
3. Gomez-Guillen M. C., Gimenez B., Lopez-Caballero M. E., et al. Functional and bioactive properties of collagen and gelatin from alternative sources: a review. Food Hydrocolloids.–25. 2011.– P. 1813–1827. DOI: 10.1016/j.foodhyd.2011.02.007.
4. Banerjee P., Suguna L., Shanthi C. Wound healing activity of a collagen-derived cryptic peptide. Amino Acids.– 47. 2015.– P. 317–328. DOI: 10.1007/s00726–014–1860–6.
5. Pappas A., Hyatt G. The evaluation of collagen film applied to skin defects in mice. Surg forum.– 10.1960.– P. 844–846.
6. Abbenhaus J. I., Donald P. The use of collagen grafts for replacement of major skin loss. Laryngoscope.– 81(10). 1971.– P. 1650–1651. DOI: 10.1288/00005537–197110000–00010.
7. Peacock E. E. J. R., Seigler H. F., Biggers P. W. Use of tanned collagen sponges in the treatment of liver injuries. Ann Surg.– 161(2). 1965.– P. 238–247. DOI: 10.1097/00000658–196502000–00013.
8. Khilkin A. M., Shekhter A. B., Istranov L. P., Lemenev V. L. Collagen and its application in medicine.– Moscow: Medicine, 1976.– 228 p.
9. Sychenikov I. A., Shekhter A. B., Dronov A. F. Collagenoplasty. Achievements and prospects of experimental surgery and anesthesia.– 2. 1974.– P. 25–31.
10. Sychenikov I. A., Aboyants R. K., Dronov A. F. etc. Collagenoplasty in medicine.– Moscow: Medicine, 1978.– 256 p.
11. Joseph Francis P. J., Arun K. J., Navas A. A. and Joseph I. Biomedical Applications of Polymers -An Overview. Curr. Trends Biomed. Eng. biosci.– 15(2). 2018.– P. 44–45.
12. Mansour H. M., Sohn M., Al-ghananeem A., Deluca P. P. Materials for Pharmaceutical Dosage Forms: Molecular Pharmaceutics and Controlled Release Drug Delivery Aspects. Int. J. Mol. sci.– 11. 2010.– P. 3298–3322.
13. Nair L. S., Laurencin C. T. Biodegradable polymers as biomaterials. Progress in Polymer Science.– 32(8––9). 2007.– P. 762–798.
14. Bolshakov I. N., Eremeev A. V., Cherdantsev D. V., Kaskaev A. V., Kirichenko A. K., Vlasov A. A., Sapozhnikov A. N. Biodegradable wound dressings based on polysaccharide polymers in the treatment of ex-

tensive burn injury (clinical studies). Problems of reconstructive and plastic surgery.– 3(38). 2011.– P. 56–62.

15. Radjabov O. I., Gulyamov T., Turaev A. S. Collagen medical, obtaining and research // Uzbek chemical journal. Special issue.2011.– P. 94–97.
16. Radjabov O. I., Turaev A. S., Gulmanov I. D., Otajanov A. Yu., Azimova L. B. Obtaining Collagen and Morphological Studies of Injection Solution on Its Basis. International Journal of Materials and Chemistry.– 12(3). 2022.– P. 39–43. DOI: 10.5923/j.ijmc.20221203.01.

Contents